

The Effect of Entrapped Laminin-111 in Three-dimensional Polyethylene Glycol Gels on
the Behavior of Nucleus Pulposus Cells from the Intervertebral Disc

by

Donna Phu

Department of Biomedical Engineering
Duke University

Date: _____

Approved:

Lori A. Setton, Supervisor

Jun Chen

Farshid Guilak

Thesis submitted in partial fulfillment of
the requirements for the degree of Master of Science in the Department of
Biomedical Engineering in the Graduate School
of Duke University

2010

ABSTRACT

The Effect of Entrapped Laminin-111 in Three-dimensional Polyethylene Glycol Gels on
the Behavior of Nucleus Pulposus Cells from the Intervertebral Disc

by

Donna Phu

Department of Biomedical Engineering
Duke University

Date: _____

Approved:

Lori A. Setton, Supervisor

Jun Chen

Farshid Guilak

An abstract of a thesis submitted in partial
fulfillment of the requirements for the degree
of Master of Science in the Department of
Biomedical Engineering in the Graduate School
of Duke University

2010

Copyright by
Donna Phu
2010

Abstract

The intervertebral disc (IVD) is a fibro-cartilaginous tissue that supports and distributes loads applied to the spine. The two main tissues types of the IVD are the annulus fibrosus (AF), which is comprised of highly organized collagen fibers arranged in lamellae, and the nucleus pulposus (NP), which is a soft, gelatinous tissue in the center of the disc. IVD disorders and associated back pain may be preceded by biological and anatomical alterations in the disc, where the most significant changes are found in the NP. Disc degeneration is characterized by a decrease in cellularity and disc height, and a replacement of the immature notochordal-like cells with chondrocytic cells. Previous work in our lab has identified the expression of specific isoforms of laminin, an ECM protein found in many tissue types, and laminin receptors in the immature NP tissue. It is widely known that ECM molecules provide biological signals that regulate many cell functions, including cell adhesion, differentiation and ECM production.

The overall aim of this thesis is to incorporate specific laminin isoforms identified in the NP into a three-dimensional (3D) hydrogel and promote the synthesis of an NP-like matrix to engineer a viable NP replacement. To generate such a hydrogel, the entrapping capabilities of laminin-111 (LM-111) in polyethylene glycol diacrylate (PEGDA), agarose and alginate were first assessed through immunostaining and

confocal microscopy. Additionally, studies were performed to examine the behavior of porcine NP cells in LM-111 laden 3D hydrogels after culture for 28 days.

Findings suggest that a photocrosslinkable system, such as the PEGDA used in this study or other covalent crosslinking systems, may be necessary to maintain the structural integrity of the cell constructs for long-term culture. LM-111 promoted greater cell viability when cultured in PEGDA gels, but did not affect the production of type I and II collagen and sulfated-glycosaminoglycans in the ECM of the constructs. Additionally, after 28 days of culture, the constructs exhibited higher compressive moduli than reported literature values of native human NP tissue.

The studies presented here demonstrate that the full-length LM-111 protein can be physically entrapped in 3D hydrogels. Furthermore, LM-111 can influence NP cell survival *in vitro* when presented in a 3D environment. The results indicate that PEGDA hydrogels that present biological cues such as laminin ECM molecules may serve as versatile platform for engineering of soft, cartilaginous tissues such as the NP.

Contents

Abstract.....	iv
List of Tables.....	viii
List of Figures.....	ix
Acknowledgements	xi
1. Introduction.....	1
1.1 Structure and Function of the Intervertebral Disc.....	4
1.2 Role of Laminin in the IVD	7
1.3 Nucleus Pulposus Tissue Engineering	11
2. Laminin-111 Entrapment in Hydrogels.....	16
2.1 Introduction.....	16
2.2 Materials and Methods.....	19
2.2.1 Agarose Gel Synthesis	19
2.2.2 Alginate Gel Synthesis.....	20
2.2.3 Polyethylene-Glycol (PEGDA) Gel Synthesis	21
2.2.4 Immunostaining Laminin-111.....	21
2.3 Results.....	23
2.4 Discussion.....	24
2.5 Conclusion.....	28
3. Nucleus Pulposus Cell Behavior in Laminin-Containing Hydrogels	29
3.1 Introduction.....	29

3.2 Materials and Methods.....	30
3.2.1 Porcine NP Cell Isolation and Encapsulation	30
3.2.2 Cell Viability	32
3.2.3 Biochemistry	33
3.2.3.1 Dimethylmethylen Blue (DMMB) Assay.....	34
3.2.3.2 Sircol Collagen Assay	34
3.2.4 Mechanical Testing	35
3.2.5 Histology	36
3.2.5.1 Safranin-O Staining.....	36
3.2.5.2 Collagen Immunohistochemistry	37
3.2.8 Statistical Analysis	38
3.3 Results.....	38
3.2.1 Cell Viability	39
3.3.2 Extracellular Matrix (ECM) Production	40
3.3.3 Mechanical Properties.....	43
3.4 Discussion.....	44
3.4.1 Long-Term Culture in Agarose Gels	44
3.4.2 Effect of Laminin-111 on NP Cell Behavior	46
3.4.3 PEGDA-Laminin Cell Constructs for NP Tissue Replacement	48
3.5 Conclusions	51
4. Conclusions and Future Directions	53
References.....	56

List of Tables

Table 1: Hydrogel biomaterials for nucleus pulposus tissue engineering.....	15
---	----

List of Figures

Figure 1: The anulus fibrosus (AF) and nucleus pulposus (NP) region of the intervertebral disc (IVD).....	5
Figure 2: Structure and receptor binding domains of laminin isoforms, LM-111 and LM-511. α DG: alpha dystroglycan receptor; Lu: Lutheran glycoprotein receptor (CD239). Laminin receptor binding information from [39-41]......	8
Figure 3: Immunostaining for laminin-binding integrin subunits in the NP and AF tissue of immature human, porcine and rat. Cell nuclei is shown in red. Scale bars: 20 μ m [15].9	
Figure 4: Light microscopy images of NP cells attached to LM-111 coated substrates for unblocked control cells (left) and cells preincubated with α 6-blocking antibody (right) [16]......	11
Figure 5: Custom made injection mold.	20
Figure 6: Representative immunostaining images of LM-111 entrapped in 5% PEGDA, 2% agarose and 2% alginate and of each respective blank gel (gels not containing LM-111).	23
Figure 7: Mean fluorescence intensity of images immunostained for LM-111 in 5% PEGDA, 2% agarose and 2% alginate in the three different axial regions: top, middle, and bottom. Values normalized to blank controls. Data shown (mean \pm SEM) represents results from 3 independent experiments. Significant main effects between biomaterials (*, $p < 0.002$) are shown.	24
Figure 8: Live/Dead images of NP cells cultured in PEGDA gels with (bottom row) or without LM-111 (top row).	39
Figure 9: Percentage of live NP cells cultured in PEGDA gels with or without 100 μ g/ml of LM-111. Data (mean \pm SEM) show results from 4 independent experiments. * $p = 0.0025$	40
Figure 10: Representative histological images of PEGDA tissue construct with and without LM-111 and native NP tissue stained with type I and II collagen. Scale bars = 200 μ m.	41

Figure 11: Collagen content levels normalized to total wet weight of tissue construct. Data shown (mean \pm SEM) are results from 4 independent experiments.	41
Figure 12: Representative safranin-O images of A) native NP tissue, B) acellular PEGDA, C) NP cells cultured in PEGDA gels for 28 days, D) NP cells cultured in PEGDA with 100 μ g/ml of LM-111 for 28 days. Scale bars are 200 μ m.	42
Figure 13: sGAG content levels normalized to total wet weight of tissue construct. Data shown (mean \pm SEM) are results from 4 independent experiments.	43
Figure 14: Compressive modulus of PEGDA cell-constructs with and without LM-111. Data shown (mean \pm SEM) are results from 3 independent experiments	44

Acknowledgements

I would like to express immense appreciation to Dr. Lori Setton for providing me with an amazing research opportunity. She has spent a large portion of her time and patience guiding me through the duration of my experimental design and analysis and through the development of my academic and professional career. From the first time we met, she has expressed sincere interest in my personal and academic endeavors, and gave me the confidence to pursue my ambitions.

Without the guidance and enthusiasm of Aubrey Francisco, I would not have been able to achieve any of the goals that I have presented in this thesis. She has been a great mentor in the lab and even greater friend outside of the lab, and I owe her much gratitude for the positive experiences in putting together this project.

Next, I would like to thank the faculty members in my thesis committee, Dr. Jun Chen and Dr. Farshid Guilak, for taking time to provide me with the support and help throughout the revision of my thesis. Thank you to Dr. Stephen Craig, Jennifer Hawk and Donghua Xu from the Chemistry Department for generously providing me with the use of their rheometer.

Other members of the Setton and Guilak lab who have devoted much time in training and teaching me include Dr. Chris Gilchrist, Dr. Dana Nettles, Liufang Jing and Bob Nielsen. These individuals have assisted me in ways that range all across the

spectrum, from training me to use the most expensive equipment that I may ever use to helping me sort through the heaping tower of lab supplies to locate a specific reagent. Dr. Gilchrist has been especially supportive through the toughest times of my experimental work and I owe him many thanks for keeping me grounded on many occasions throughout my project.

Finally, I would like to acknowledge all of the love and support from my family, especially from Michael Mayeda who has heard all the stories of the trying times when the rheometer computer crashed or the cells were contaminated. He shares with me the joy and pride that I take in this accomplishment and I am forever grateful for all of his compassion and patience.

1. Introduction

The human intervertebral disc (IVD) is a soft tissue that lies in the space between the vertebral bodies that provides flexibility in the spine. It is responsible for dissipating energy and distributing the loads applied to the vertebral column [1]. The function of the IVD is greatly affected by the composition and organization of its extracellular matrix (ECM) components [2]. During aging and degeneration, the disc undergoes significant cell-mediated tissue remodeling including rearrangement of lamellae in the annulus fibrosus (AF) region, calcification of the vertebral endplates, and even fibrosis in the nucleus pulposus (NP) region [3]. The cells of the immature NP are larger, contain an extensive cytoskeleton and are highly vacuolated when compared to the chondrocytic cells found in the mature NP tissue. They are believed to be derived from the notochord [4-7]. Many research groups have focused on identifying unique cell markers of these notochordal NP cells, but the role of these cells during disc degeneration is unclear. It is known that these notochordal cells have been shown to be an essential factor for NP tissue regeneration because they produce an ECM that is rich in proteoglycan content [5]. The most notable changes to the disc occur in humans soon after birth in the NP tissue, where the notochordal cells become replaced with smaller chondrocyte-like cells that migrate from either the surrounding AF or endplate tissue [8]. The mechanism and functionality behind the disappearance of these notochordal

cells in the NP remains unclear, but the loss of these notochordal cells coincides with the onset of disc degeneration [3, 8]. With the disappearance of notochordal NP cells, matrix synthesis is greatly altered, leading to a subsequent loss of normal IVD function.

Therefore, treatments for disc degeneration may greatly benefit from a greater understanding the factors that influence this shift in cell population in the NP region of the disc.

Like many tissue types, the structure and composition of the ECM of the NP is an important regulator of interactions between the cells and their environment. Many studies have identified specific integrins that interact with various ECM proteins such as collagen, fibrinogen and laminin [9]. Integrins are important cell-matrix adhesion transmembrane molecules that communicate the extracellular content to the cytoskeleton inside the cells. Integrins regulate cell functions such as signaling, gene expression, proliferation, differentiation and apoptosis [10]. Studies have shown that integrin expression may change with the onset of certain pathologies such as osteoarthritis in articular cartilage [11-13] and herniated disc in the IVD [14].

Furthermore, the expression of certain laminin subunits, including the $\alpha 5$ and $\gamma 1$ chain, in the NP of younger human patients (2-12 years) are not found in older subjects (35 years) [15]. The results presented from these studies may offer valuable insight into the role of cell-matrix interactions in regulating the progression of disc degeneration and

aging. Furthermore, many studies done in our lab have demonstrated differential expression of integrin subunits in NP and AF tissue, with a higher expression of laminin-111 (LM-111) and laminin-511 binding integrins in the NP tissue [15-17]. These results suggest an important role of LM-111 and laminin-511 in maintaining a NP cell phenotype.

The overall hypothesis of this work is that the incorporation of important ECM proteins, such as LM-111, into a three-dimensional (3D) hydrogel will promote cell viability and synthesis of an NP-like matrix to engineer a viable NP replacement. Due to poor protein adsorption and cell adhesion properties, polyethylene-glycol (PEG) offers a suitable blank three-dimensional environment on which the specific interactions between cells and entrapped ECM ligands can be studied in a 3D environment. When PEG is functionalized with methacrylate (PEGDM) or acrylate groups (PEGDA), it can be induced to crosslink through radical polymerization upon the addition of an appropriate initiator and exposure to ultraviolet radiation to form a 3D gel [18]. The wavelength of UV light used in these studies is within the approved range of the FDA for clinical use [19]. Many groups have demonstrated that the photoinitiator used in these studies is not toxic to many mammalian cell types [20-22]. In these studies, the ability of PEGDA to entrap full-length laminin-111 is compared against that of selected hydrogel biomaterials that are commonly used in IVD tissue engineering efforts, such as

agarose and alginate [23-29]. In addition, cells isolated from porcine NP tissue, which maintain a high population of notochordal-like cells even in maturity, were entrapped in the ECM-presenting hydrogels and their behavior was investigated to determine the role of laminin-111 in regulating cell-matrix interactions, cell phenotype, matrix productions and the whole construct mechanical properties.

1.1 Structure and Function of the Intervertebral Disc

In humans, there are a total of 23 intervertebral discs (IVD) that increase in size from the cervical to the lumbar regions and serve as joints between the vertebrae to provide flexibility and controlled mobility of the spine. The IVD is comprised of two main tissue types: the annulus fibrosus (AF) and nucleus pulposus (NP) (Figure 1). The top and bottom of the IVD articulates with a thin, vascular layer of hyaline cartilage known as the cartilaginous endplates, which is the tissue through which nutrients diffuse to reach the avascular IVD [30]. Similar to other hyaline cartilaginous tissues, the EPs are composed of rounded chondrocytes [3].

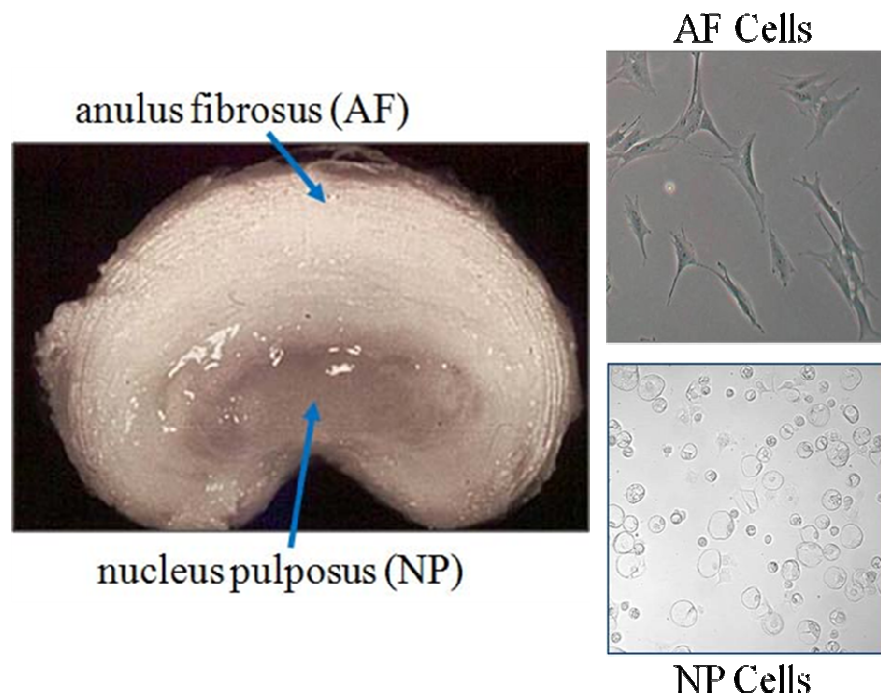


Figure 1: The anulus fibrosus (AF) and nucleus pulposus (NP) region of the intervertebral disc (IVD).

The AF tissue is a fibrous, concentric tissue that is mainly composed of water (60-70% of its wet weight) and collagen type I (50-60% of its dry weight) [30]. The AF tissue is comprised of sheets of collagen fibers aligned in concentric lamella that alternate between adjacent lamella by approximately 30° with respect to the transverse plane [31]. The AF tissue is populated with fibroblast-like cells that elongate along the direction of the collagen fibers [3].

In each disc, the lamella of the AF enclose the highly hydrated NP tissue (70-90% water) in the center of the IVD [30]. Proteoglycans constitute approximately 65% the dry weight of the NP tissue, which allows it to effectively imbibe water. Interspersed between the proteoglycan aggregates are randomly-oriented, nonfibrillar collagens, such as type II collagen [30]. Unlike the AF tissue, the cell population of the NP consists of two main cell types, the larger notochordal cells found in immature tissues and the smaller chondrocyte-like cells. The cell types found in the NP vary with age, which may help explain the changes in the disc's overall structure during and after degeneration. Studies have shown that these immature notochordal cells are more active in synthesizing proteoglycans than the chondrocytic cells, which indicates that the immature cells may be important for the maintenance of the gelatinous NP structure found in the earlier stages in life [32]. Additionally, some studies have indicated that the introduction of notochordal cells into an older patient may help maintain a healthy NP phenotype and even may delay the onset of IVD degeneration [33]. Notochordal cells may even secrete soluble factors that influence other cell types to synthesize a proteoglycan-rich matrix [34]. These findings suggest that a better understanding of the factors that maintain and prolong the presence of notochordal cell phenotype may be critical for treatment of disc degeneration.

1.2 Role of Laminin in the IVD

The extracellular matrix (ECM) is an important regulator of cell functions, including cell survival, apoptosis and phenotype maintenance. In the immature intervertebral disc (IVD), the nucleus pulposus (NP) is populated by highly vacuolated cells believed to be derived from the notochord. They usually appear in clusters and stain intensely for cytoskeleton elements, indicating the cell-cell interactions may be critical for proper cell function [35-38]. As the disc matures and ages, the cell population shifts to exhibit a more chondrocyte-like phenotype, which is smaller and less round than the immature NP cell. It is unknown whether these cells are a result of a differentiation pathway or of migration from the cartilaginous endplates and/or annulus fibrosus (AF) [15].

Laminin is a large, cross-shaped heterotrimer protein that is commonly found in the ECM of many tissue types. In mammals, fifteen known different laminin isoforms exist from combinations of α -chains ($\alpha1 - \alpha5$) with the β -chains ($\beta1 - \beta3$) and γ -chains ($\gamma1 - \gamma3$), where each laminin isoform contains one α , β , and γ chain [15]. Different tissues express specific laminin isoforms that vary with the type and developmental stage of the tissue. Laminin has been shown to interact with cells through several integrins receptors, including $\alpha6\beta1$, $\alpha6\beta4$, $\alpha3\beta1$, and $\alpha7\beta1$, and non-integrin receptor proteins including Lutheran blood group glycoprotein (CD239), α -dystroglycan and

tetraspanin (CD151) [15]. Knowledge of the specific laminin isoforms and their associated receptors expressed in immature NP tissue is of great interest for this project. Figure 2 shows a schematic of the two laminin isoforms of most interest to this project, laminin-111 (LM-111) and laminin-511 (LM-511).

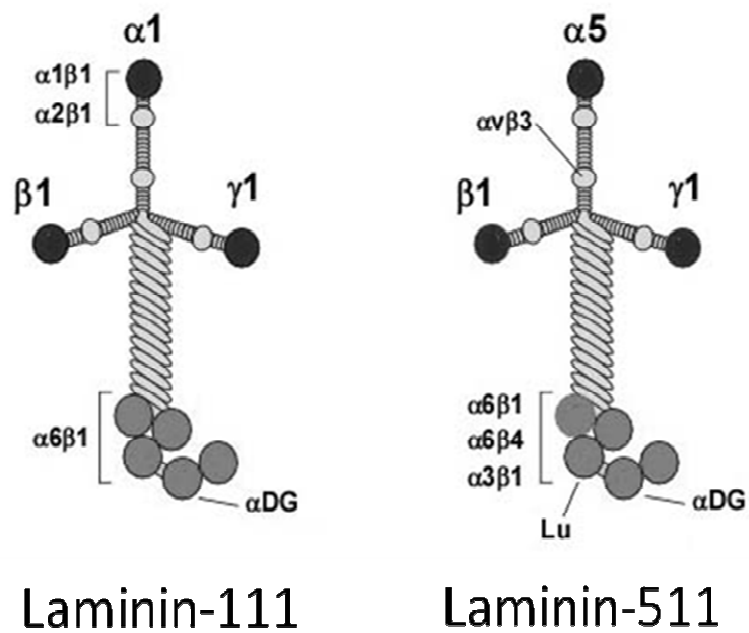


Figure 2: Structure and receptor binding domains of laminin isoforms, LM-111 and LM-511. αDG : alpha dystroglycan receptor; Lu: Lutheran glycoprotein receptor (CD239). Laminin receptor binding information from [39-41].

Previous research in our lab has identified the specific expression of the $\alpha 6 \beta 1$ and $\alpha 6 \beta 4$ integrins in the IVD, which interact with LM-111/121 and LM-511/521, respectively [17]. Research in our lab has revealed specific expression of the $\alpha 3$, $\alpha 6$, $\beta 1$ and $\beta 4$ integrin subunits in the immature NP compared to the AF in humans, porcine and rat tissues (Figure 3) [15]. Laminin receptor CD239 and laminin-binding protein CD151 are also expressed in higher levels in human NP compared to AF tissue [15].

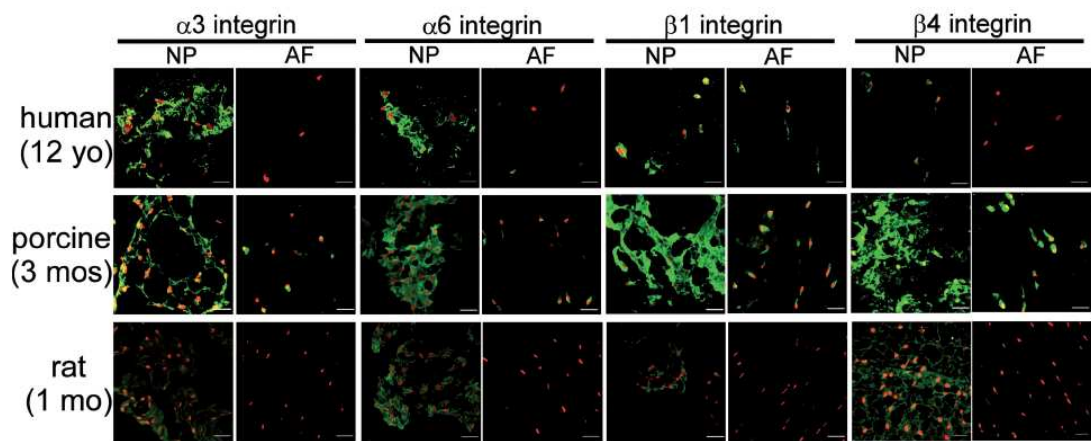


Figure 3: Immunostaining for laminin-binding integrin subunits in the NP and AF tissue of immature human, porcine and rat. Cell nuclei is shown in red. Scale bars: 20 μ m [15].

In addition, Chen *et al.* identified higher expression of the $\alpha 5$ laminin chain in both immature rat and porcine NP tissue than in the AF tissue. Additionally, they found a higher expression of the $\alpha 1$ laminin chain in the AF tissues than in NP tissue. These results suggest that LM-511/521, which are both formed from the $\alpha 5$ and $\gamma 1$ chains, may be uniquely present in the NP, whereas LM-111/211 formed from the $\alpha 1$ and $\gamma 1$ chains may be in the AF [15]. However, a separate study demonstrated greater cell adhesion to substrates coated with the full-length LM-111 protein for porcine NP cells than for AF cells [16]. Furthermore, blocking integrin subunits $\alpha 6$ and $\beta 1$ that have been shown to interact with LM-111 [17], greatly reduced NP cell adhesion [16]. Specifically, blocking the $\alpha 6$ integrin inhibited larger cells (25-30 μm) from adhering to LM-111 coated substrate (Figure 4). This is of particular importance because the larger cells may be the notochordal cells that are responsible for synthesizing a proteoglycan-rich ECM. Another study sorted the larger, vacuolated NP cells (25-30 μm) from the smaller ones (10-20 μm), and demonstrated a much higher expression of the $\alpha 1$, $\alpha 6$ and $\beta 1$ integrin subunits in the larger NP cells than in the smaller ones [42]. These results suggest an important role for LM-111, and possibly LM-511, isoforms in not only promoting NP cell adhesion, but also maintaining the immature NP cell phenotype.

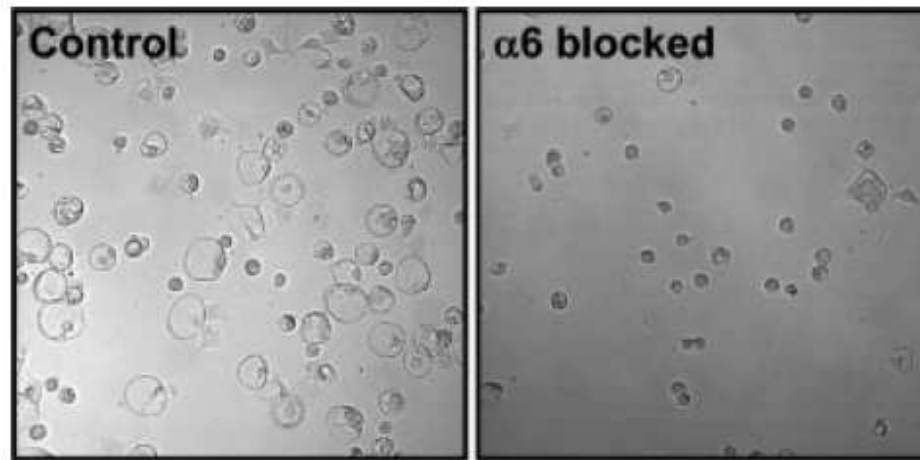


Figure 4: Light microscopy images of NP cells attached to LM-111 coated substrates for unblocked control cells (left) and cells preincubated with $\alpha 6$ -blocking antibody (right) [16].

1.3 Nucleus Pulposus Tissue Engineering

Degeneration of the intervertebral disc (IVD) is the most expensive healthcare problem in the United States today. It affects approximately 8 of 10 people worldwide, and usually begins between the ages of 10 and 20 in humans [2]. In many cases, a degenerated disc will result in a herniated disc, where the nucleus pulposus (NP) is extruded out of the disc space. The pain associated with disc degeneration is caused by a pinching in the sciatic nerve, which begins in the low back and runs through the lower limbs [43]. The most common treatment for a herniated disc is a surgical procedure called spinal fusion, in which the two vertebrae flanking the degenerated disc are fused together via a bone graft to stabilize the joint and alleviate pain [44]. Unfortunately, this

procedure results in a significant loss in mobility and many cases have reported degeneration and altered biomechanics in other levels of the spine [2]. A promising alternate treatment is using tissue engineering techniques to either repair or completely replace the nucleus pulposus (NP) tissue, where disc degeneration is believed to originate.

The most noticeable change that occurs in disc degeneration is the significant decrease in cell viability in the NP tissue [43]. Many research groups have investigated the method of injection of cells into the NP space to retard the rate of disc degeneration. One study found that reinsertion of autologous NP cells after *in vitro* co-culture with autologous AF cells into the patient resulted in a decrease in degeneration rate as well as an increase in collagen type II synthesis [45]. Other studies have co-cultured NP cells directly with mesenchymal stem cells (MSCs) *in vitro*, as they have been shown to serve as feeder cells that secrete essential factors for the growth of a variety of cell types [46]. Another study revealed that MSCs can also induce NP cells to increase the expression of growth factors, particularly TGF- β and insulin growth factor (IGF), which may be beneficial for proper ECM deposition [47]. The disadvantage of using autologous NP cells is that cell numbers might not be high enough to harvest from a degenerated disc and expansion in culture is difficult. Furthermore, explanting cells from a patient with a disc that is already lacking in cell density may cause more damage to the tissue.

While cell-based therapies have shown great efficacy in slowing down the rate of disease progression for both *in vitro* and *in vivo* studies, the most significant limitation is that these therapies can only be applied at most for moderate levels of disc degeneration. In many cases of disc degeneration and disease, the environments in which the cells will be injected are too harsh to foster any cell growth and functionality, including new cells that are injected into the space. In addition, these therapies may only offer a temporary restoration of normal IVD function, and it does not actually address the need for long term stability. Furthermore, the cells may leave the compromised disc space before any therapeutic effect is achieved. To overcome these obstacles, a cell carrier is needed.

To fully restore the mechanical and biological functions of the degenerated IVD, a comprehensive tissue engineered NP that includes cells seeded in a 3D scaffold environment may be necessary. Hydrogels have proven to be a class of materials with great potential for NP replacement due to their ability to imbibe water and swell and shrink in response to external loads [48, 49]. These properties allow hydrogels to mimic the highly hydrated nature of the NP tissue. The hydrogel material can protect the cells from the acidic environment of the degenerated disc, provide a platform to foster tissue repair and partially restore the mechanical function of the NP. To date, a variety of hydrogels, both synthetic and natural, have been investigated for replacement of the soft, cartilaginous tissues such as the IVD (Table 1). Many research groups have

demonstrated promising results for their hydrogel system to maintain the correct cell morphology, deposit an appropriate ECM with high proteoglycan content, and exhibit functional mechanical properties. O'Halloran and Pandit provide a detailed review of the some of the recent research efforts to tissue engineer the intervertebral disc [2].

Most of these studies listed in Table 1 did not focus on the effect of their hydrogel biomaterial to influence NP cell phenotype and function. This is mainly due to the lack of knowledge about the biological description and function of the immature NP cell. Several studies have demonstrated that notochordal cells found in immature NP tissue may greatly reduce the rate of disc degeneration and even foster the repair and regeneration of damaged NP [4, 5]. Thus, it is of great interest for future investigations to develop a comprehensive understanding of the factors that can maintain a healthy NP cell phenotype. One of the main objectives of the studies presented here is to study the effect of LM-111 on the phenotype and function of NP cells isolated from immature porcine spine in a 3D hydrogel environment.

Table 1: Hydrogel biomaterials for nucleus pulposus tissue engineering.

Hydrogel Biomaterial	Major Findings	Reference
Agarose	<ul style="list-style-type: none"> • High sGAG production • Rounded NP cell morphology 	[25-27]
Alginate	<ul style="list-style-type: none"> • AF cells expressed type I collagen • NP cells expressed type II collagen • Compressive modulus was less than native NP tissue 	[23]
Alginate	<ul style="list-style-type: none"> • Ionically crosslinked gels lost structural integrity • NP cells cultured in photocrosslinked gels had higher cell viability 	[24, 50]
Cellulose	<ul style="list-style-type: none"> • Rounded NP cell morphology • Expressed proteoglycans 	[51]
Chitosan	<ul style="list-style-type: none"> • NP cells remained viable up to 20 days in culture • Supported sGAG production and accumulation 	[52]
Collagen	<ul style="list-style-type: none"> • Proteoglycan synthesis and accumulation • Higher water content in type II collagen than in type I collagen 	[53]
Hyaluronan	<ul style="list-style-type: none"> • Acellular hyaluronan based hydrogels demonstrated similar mechanical properties to human NP tissue 	[54]

2. Laminin-111 Entrapment in Hydrogels

2.1 Introduction

Because the extracellular matrix (ECM) can influence cell behavior through specific receptor-ligand interactions, the incorporation of ECM components into a biomaterial scaffold may enhance the survival and functionality of cells in the construct. Many groups have utilized hydrophilic hydrogels to provide a 3D environment that closely resembles the soft mechanical properties of most tissues for cell culture. However, many of these hydrogel materials, such as polyethylene glycol (PEG), do not present direct binding sites for cell adhesion which may be important in promoting normal cell function. Thus, the biomaterial alone is not sufficient to promote proper cell function. This has led to the incorporation of biological cues such as full length ECM proteins or peptides that represent important binding domains, such as RGD in fibronectin, laminin, collagen type I and type IV or IKVAV and YIGSR in laminin [55, 56].

The presentation of ligands on 2D substrates enhanced functional outcomes, such as neurite extension in dorsal root ganglion cells [57-59] or insulin production in β -islet cells [60, 61], compared to nonfunctionalized surfaces. More interest has been focused on presenting these peptide sequences in a 3D environment, as it provides a microenvironment that more closely resembles that of the native tissues. For example,

one group demonstrated that neurite spread was significantly greater in 3D agarose gels that have been modified to present cell-binding domain peptide sequences YIGSR and PEPPIX than in unmodified agarose gels [55]. These peptides were covalently attached to the hydroxyl groups in agarose and the N-terminus of the peptide chain through a 1,1 carbonyl-diimidazole (CDI) linker. Another group encapsulated β -islet cells in polyethylene-glycol diacrylate (PEGDA) modified with laminin-derived peptide sequences and demonstrated a reduction in percentage of apoptotic cells and increase in insulin secretion for cells encapsulated in a peptide-presenting environment over those in a blank PEGDA gel [56].

Compared to full-length proteins, small peptide sequences incorporated into the biomaterial scaffold may limit the interference of nutrient and cytokines diffusion within the 3D network. However, the functional effects of the presented ECM component may be compromised when choosing to use an active domain compared to the whole protein. Bellamkonda *et al.* demonstrated the full-length laminin protein can be coupled to agarose with the same chemistry used to attach the laminin peptide sequences [62]. Furthermore, the full laminin protein enhanced neurite extension more than the peptides did [62]. Similarly, encapsulating the whole proteins of collagen type IV and laminin improved glucose-stimulated insulin production in β -cells cultured in a 3D PEGDA gel more than the peptide sequences did [22, 63]. Other groups have succeeded

in covalently coupling large ECM proteins such as fibrinogen that have been modified with a thiol group to PEGDA monomers [21, 64]. These results indicate the benefits for utilizing full-length proteins to promote the most functionality in tissue engineered constructs.

The main objective of this project is to promote NP cells to synthesize an NP-like matrix by presenting LM-111, an ECM molecule that has previously been demonstrated to influence NP cell attachment *in vitro*, in a 3D hydrogel environment. In this study, LM-111 was physically entrapped in the biomaterials and no covalent crosslinks were used to immobilize the protein. Since physical entrapment is a much simpler process as it avoids the necessity of chemically modifying the protein, it is of interest to first evaluate the suitability of these laminin-containing biomaterials as a scaffold for NP tissue engineering strategies. The first goal is to verify the entrapment and characterize the distribution of LM-111 in three different hydrogels biomaterials. The ability of PEGDA, agarose and alginate to entrap the full-length LM-111 protein was assessed to evaluate the potential of these hydrogel biomaterials as a viable material for nucleus pulposus regeneration.

2.2 Materials and Methods

2.2.1 Agarose Gel Synthesis

Low melt PCR agarose (BioRad; Hercules, CA) was dissolved in 1X phosphate buffered saline (PBS) (Invitrogen; Carlsbad, CA) solution to a final concentration of 2% (w/v). The solution was placed in a rotating oven at 60°C for 30 minutes. Following heating, a 1 mL syringe with a 21½ G needle was used to inject the gel solution into custom-made injection molds (Figure 5). For blank agarose gels, the solution was immediately injected into the molds and allowed to completely gel upon cooling down to temperature. For gels containing LM-111 (LM) (Trevigen; Gaithersburg, MD), LM-111 was added once the gel solution reached 40°C to a final concentration of 100 µg/mL, subsequently injected into molds and allowed to completely cool down to room temperature. After removing gels from the molds, a 5-mm biopsy punch was used to obtain cylindrical discs 2 mm in height.

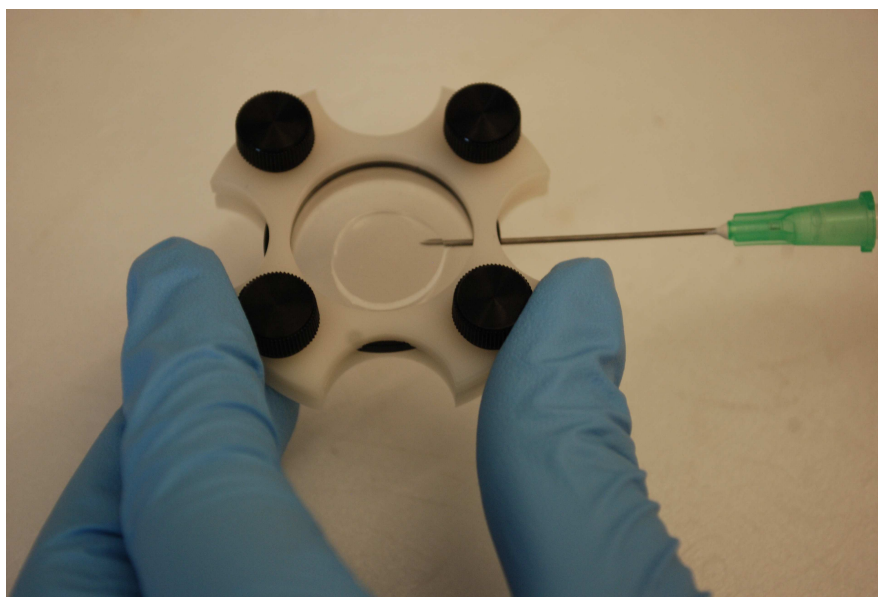


Figure 5: Custom made injection mold.

2.2.2 Alginate Gel Synthesis

Sodium alginate (Sigma; St. Louis, MO) was dissolved in 1X PBS for a final concentration of 2% (w/v). The solution was allowed to stir for 1 hour at room temperature. For LM containing gels, LM was added to the solution after 1 hour of stirring to a final concentration of 100 $\mu\text{g/mL}$ and stirred for an additional ten minutes. LM was added after initial stirring to avoid unnecessary shearing of the protein. A 1 mL syringe and 21½ G needle was used to inject each gel solution into injection molds. The entire injection mold was completely submerged in a 102 mM calcium chloride (Sigma) polymerizing solution containing 100 mM sodium chloride (Fisher Scientific; Waltham,

MA) and 50 mM HEPES (Sigma) overnight. After removing gels from the molds, 5-mm biopsy punch was used to obtain cylindrical constructs 2 mm in height.

2.2.3 Polyethylene-Glycol (PEGDA) Gel Synthesis

Irgacure 2959 (Ciba Co.) was dissolved in deionized water to a final concentration of 1%. The solution was sonicated for 10 minutes and subsequently incubated in a rotating oven at 60°C for 1 hour to solubilize the Irgacure 2959 before use. To obtain blank PEGDA gels, a 10 kDa PEGDA-diacrylate (PEGDA) (PEGWorks; Winston Salem, NC) was dissolved in 1X PBS to obtain a final concentration of 5% (w/v). Irgacure was added to the solution to a final concentration of 0.1% (w/v). For LM-containing gels, LM was added to a final concentration of 100 µg/ml. A 1 mL syringe and 21½ G needle was used to inject each gel solution into injection molds. The molds were placed under UV light (365 nm, 3000-4000 µW/cm²) for 8 minutes. After removing gels from the molds, 5-mm biopsy punch was used to obtain cylindrical constructs 2 mm in height.

2.2.4 Immunostaining Laminin-111

Each construct was embedded in OCT medium immediately after it was synthesized and flash-frozen in liquid nitrogen. A cryostat was used to obtain 20-µm sections from the top, middle and bottom regions of the constructs. The sections were stored at -20°C until the day of analysis. Samples were then oven-dried at 60°C for 30

minutes, rehydrated in 1X PBS, and blocked with 10% goat serum containing sodium azide. The samples were then subsequently labeled with 1:50 dilution of LM-111 primary antibody (Sigma) for 45 minutes and a 1:200 dilution of AlexaFluor goat anti-rabbit 488 (Invitrogen) for 20 minutes. Samples were rinsed twice with 1X PBS after each incubation. Samples were then mounted in mounting medium and allowed to dry for 1 hour before imaging.

Images of samples were obtained using an inverted laser scanning confocal microscope (Zeiss LSM 510, Plan-Neofluar 10X objective, confocal slice thickness = 20 μ m). For each construct, three images were taken of each of three sections. The mean fluorescent intensity was measured using a Nikon image analysis software (Nikon NIS-Elements BR; Melville, NY). To account for variation in staining procedure between experiments, the mean intensity of sections containing laminin was normalized against the sections from the blanks of each respective biomaterial. For each construct, nine images were averaged to obtain one data point per experiment. Data are presented as the mean \pm SEM ($n = 3$). A one-way ANOVA was used to determine differences in LM-111 entrapment. A Tukey's *post-hoc* analysis was used to determine differences amongst the groups at a significance level of 0.05. Statistical analyses were performed using JMP software (SAS Institute; Cary, NC).

2.3 Results

After gelation, all of the LM-111 containing gels exhibited detectable levels of immunostaining for all biomaterials used. A qualitative analysis of the images showed that the LM-111 was evenly distributed transversely within each section in the agarose and alginate gels (Figure 6). In the PEGDA gels, LM-111 appeared to aggregate primarily on the edges of each section, with few aggregates seen towards the center of each section.

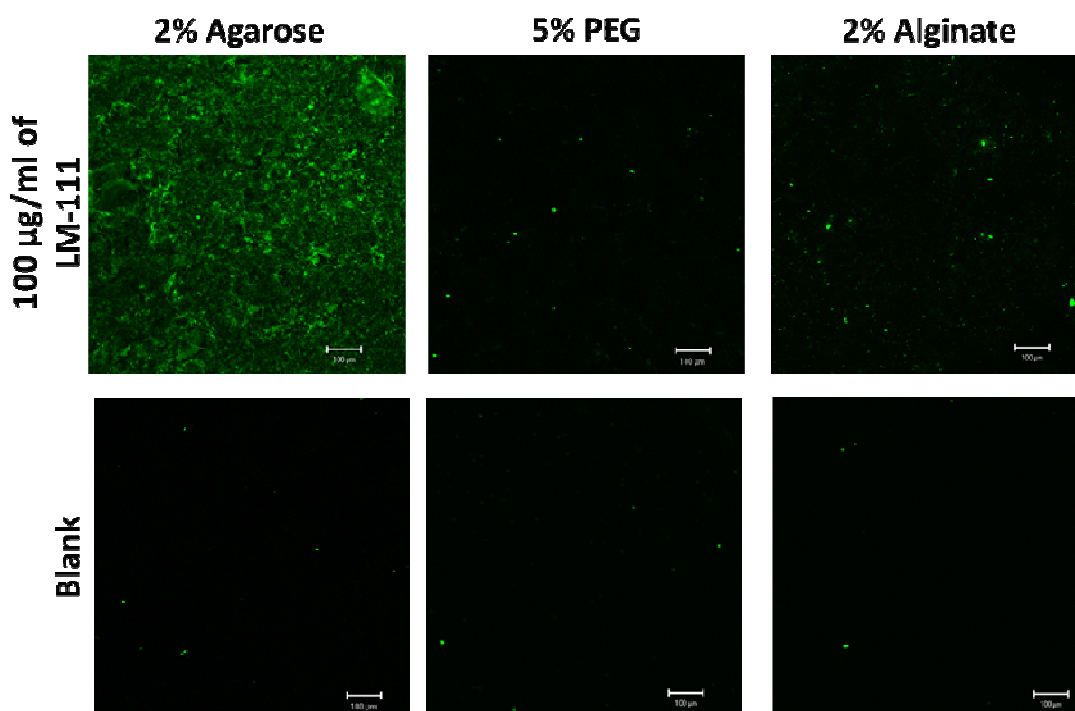


Figure 6: Representative immunostaining images of LM-111 entrapped in 5% PEGDA, 2% agarose and 2% alginate and of each respective blank gel (gels not containing LM-111).

Quantifying the mean fluorescence of the images revealed no significant difference in laminin distribution in the axial axis (from bottom to the top of the cylindrical constructs; $p > 0.99$; Figure 7). In addition, agarose entrapped a significantly higher amount of LM-111 than both the PEGDA and alginate gels ($p < 0.002$; Figure 7).

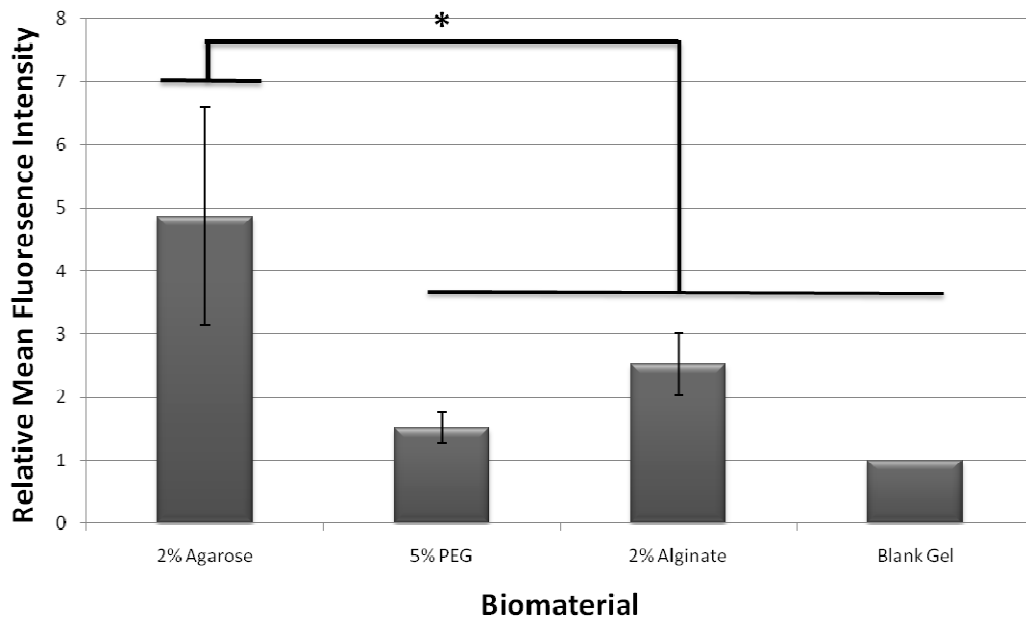


Figure 7: Mean fluorescence intensity of images immunostained for LM-111 in 5% PEGDA, 2% agarose and 2% alginate in the three different axial regions: top, middle, and bottom. Values normalized to blank controls. Data shown (mean ± SEM) represents results from 3 independent experiments. Significant main effects between biomaterials (*, $p < 0.002$) are shown.

2.4 Discussion

ECM-presenting hydrogels provide a cell culture method to mimic the architecture and composition of native tissues in a 3D environment. Various groups

have demonstrated methods to encapsulate small molecules and peptide sequences in hydrogels [22, 55, 59, 65-67]. Some studies have shown that it is possible to encapsulate proteins as large as 800 kDa in PEGDA hydrogels [63]. In this present study, immunostaining images revealed that agarose, alginate and PEGDA were all capable of entrapping the full-length LM-111 protein to varying degrees. Agarose demonstrated the highest amount of entrapped LM-111 than both alginate and PEGDA. Since it is hypothesized that LM-111 may be important for regulating NP cell behavior to synthesize an NP-like ECM, a biomaterial that can entrap abundant amount of protein is desirable. This increase concentration of entrapped protein in agarose may be due to the large number of hydroxyl groups present in the polymer chain which can form hydrogen bonds with various amino acids in the LM-111 protein sequence. However, this is unlikely since alginate also presents many hydroxyl groups capable of forming hydrogen bonds with LM-111.

It is possible that the mechanism of polymerization can affect the amount and distribution of LM-111 within the gels. Immunostaining images suggest that the LM-111 distributed evenly within the agarose gel. In contrast, LM-111 appears to form aggregates in both PEGDA and alginate gels. Both alginate and PEGDA require an initiator to polymerize and form a gel. The self-polymerization of agarose may improve protein entrapment because it can form a gel in one step rather than through a

propagation of steps. Agarose gels are formed through glycosidic linkages between a hemiacetal group on the anomeric carbon and a hydroxyl group from another monomer. It is possible that certain amino acids, such as serine or threonine, in LM-111 can form similar linkages to agarose monomers. This may explain the even distribution of LM-111 in agarose than in alginate or PEGDA. Although alginate is a polysaccharide, glycosidic linkages are not seen in alginate because crosslinks between monomers are formed using divalent cations. Further analysis will be required to determine how LM-111 interacts with each polymeric material. Additionally, further experimentation will assess the biofunctionality of LM-111 after incorporation into each of the biomaterials.

Future studies will also need to investigate the diffusion properties of LM-111 out of these hydrogels over time. All gels were flash frozen and sectioned immediately after gelation, which provided little opportunity for the LM-111 protein to diffuse out of the hydrogels. However, it is still important to characterize the diffusion properties of LM-111 out of these 3D hydrogels since most *in vitro* tissue culture studies will be carried out over a span of days. Several studies have characterized the diffusion properties of small proteins out of PEGDA gels of different molecular weights and weight concentrations [18, 22]. Increasing the molecular weight of the PEGDA monomers leads to a larger mesh size within the polymer network, and subsequently greater diffusion of small molecules out of the membrane [18]. This study suggests that

it is unlikely LM-111 is diffusing out of the PEGDA network due to its large molecular weight (~800 kDa). The results from these diffusion studies are important for understanding the encapsulation of protein molecules within the PEGDA network. Since a higher intensity of LM-111 staining was seen on the edges of the PEGDA gels, it is likely that the LM-111 is being pushed towards the edges of the gel during the free radical polymerization process. Since the polymer solution was immediately placed under UV light after injection into the mold, it is unlikely that the localization of LM-111 at the edges is due to an uneven distribution of the photoinitiator in the solution. In contrast to the findings presented here, another group reported an even distribution of LM-111 encapsulated in 10% (w/v) PEGDA gels [63]. In this study, a 5% (w/v) PEGDA gel was used. This discrepancy suggests that the crosslinking density may affect protein distribution when encapsulated in the same biomaterial. Using a PEGDA monomer with a molecular weight higher than 10 kDa may increase the mesh size and improve the LM-111 entrapping properties of PEGDA and may also increase diffusion of nutrients throughout the gel. Future studies will need to investigate the role of molecular weight and crosslinking density on protein entrapment to determine the optimal system for maximizing protein content in 3D hydrogels.

2.5 Conclusion

The goal of this experiment was to compare the entrapping capabilities of three different hydrogel biomaterials that are commonly used for engineering soft, cartilaginous tissues: agarose, alginate and PEGDA. The ability of the material to entrap LM-111 may be due to an intrinsic property of the polymer itself, such as increased sites for hydrogel bonding, or the method of polymerization. The results from this study suggest that agarose may provide a more suitable 3D scaffold in regards to entrapping protein than either alginate or PEGDA. However, it is necessary to evaluate the biofunctionality of LM-111 following entrapment in each biomaterial. Since there was no significant difference between LM-111 concentration in alginate and PEGDA, further experiments investigating NP cell behavior will focus on agarose and PEGDA.

3. Nucleus Pulposus Cell Behavior in Laminin-Containing Hydrogels

3.1 Introduction

An essential function of NP tissue is to synthesize high levels of proteoglycans in the extracellular (ECM) in order to imbibe water and redistribute loads applied to the spinal column. *In vivo*, immature nucleus pulposus (NP) cells are organized in clusters in a soft, highly hydrated ECM environment. These cell clusters are thought to be important for promoting critical cell-cell interactions [68, 69]. Additionally, the immature NP tissue shows differential staining of laminin chains, integrins and laminin-binding receptors from AF cells and also from the smaller, chondrocytic NP cells that are found in the disc space later in life. Degeneration of the disc is associated with loss of proteoglycan and water content and the disappearance of the immature NP cell population. These findings suggest that the presence of certain ECM components, such as laminin, may be important in promoting cell adhesion, maintaining a notochordal-like phenotype, and inducing cells to synthesize an ECM that mimics that of the native NP microenvironment.

Several studies using inert hydrogels have demonstrated the ability of NP cells to produce an ECM that contains some glycosaminoglycan (GAG) content and type II collagen, both found in the native NP ECM (Table 1) [23, 24, 26, 29, 50, 51]. Most of these studies focused on the effect of the biomaterial itself to regulate normal NP cell function.

The study presented here is one of the first to incorporate biological cues such as LM-111 into three-dimensional hydrogels for NP tissue engineering. The effect of LM-111 on NP cell behavior was assessed in PEGDA, which provides a blank 3D environment to study the specific interactions between the ECM molecule and the cells, and agarose, which has is a naturally-derived polymer that resembles the polysaccharide structure in native tissues and was shown to physically entrap the highest amount of LM-111 (Section 2). Based on results from Chapter 2, it was hypothesized that agarose will enhance the production of an NP-like matrix over the other scaffold conditions investigated because it is a polysaccharide that is similar to the components found in the ECM of the native tissue and entraps the highest amount of LM-111 (**Hypothesis 3.A**). Furthermore, the incorporation of key ECM components, such as LM-111, into the hydrogel can further enhance the production of an NP-like matrix (**Hypothesis 3.B**) and promote cell proliferation and survival (**Hypothesis 3.C**) over the course of a 28 day culture.

3.2 Materials and Methods

3.2.1 Porcine NP Cell Isolation and Encapsulation

Porcine spines were obtained from pigs immediately after sacrifice (Nahunta Pork Outlet; Raleigh, NC). Cells were isolated from the NP regions of the intervertebral discs (IVDs) via overnight enzymatic digestion in 37°C wash medium (Dulbecco's Modified Eagle's Medium containing High Glucose (Invitrogen; Carlsbad, CA)

containing 1.65 mL of 300X Gentamycin (Invitrogen), 5 mL of 100X Kanamycin (Sigma; St. Louis, MO), and 2 mL of 250X Fungizone (Invitrogen) with 0.08% collagenase type II (Worthington Biochemicals; Lakewood, NJ) and 0.04% pronase (Roche Applied Science, Mannheim, Germany). The remaining cell suspension was centrifuged at 400 g for 10 minutes to collect the cell pellet, and rinsed with wash medium, with this procedure repeated twice for a total of three rinses. In some cases where NP cells remained in cell clusters (viewed under light microscopy) following washing, cells were resuspended briefly (3-5 minutes) in 1X phosphate buffered saline (PBS) solution (Invitrogen). If NP cell clustering was still observed after suspension in PBS, then cells were resuspended in non-enzymatic cell disassociation buffer CellStripper (Mediatech, Manassas, VA). Following washing, cells were resuspended in culture media (Ham's F-12 media (Invitrogen) supplemented with 10% fetal bovine serum (FBS; ThermoFisher Scientific; Waltham, MA), 10 mM of HEPES (Invitrogen), 100 U/mL penicillin (Invitrogen), and 100 mg/mL of streptomycin (Invitrogen) and counted using a hemocytometer. Isolated cells were then seeded onto 804G media-coated T75 tissue culture flasks at a seeding density of 50,000 cells/cm² and cultured for 3-5 days in culture media prior to encapsulation.

On the day of encapsulation, cells were trypsinized (0.025% Trypsin/EDTA; Lonza; Walkersville, MD) and resuspended in culture media. Agarose and PEGDA powder were sterilized under germicidal UV light for 30 minutes before use. For

PEGDA gels, cells were resuspended at a density of 10×10^6 cells/mL into a 5% (w/v) PEGDA solution containing 0.1% (w/v) Irgacure. For agarose gels, the solution was allowed to stir at 60°C for 30 minutes. Cells were then resuspended in premixed agarose solution at a density of 10×10^6 cells/mL. In both cases, the polymer-cell solution was injected into a sterilized injection mold using a 1 mL syringe with a 22 ½ G needle (Figure 5). PEGDA gels were crosslinked under UV light for 8 minutes (365 nm; 3000-4500 $\mu\text{W}/\text{cm}^2$). Agarose gels were formed upon cooling to room temperature. For LM-111-containing gels, LM-111 (Trevigen) was added to the solution to a final concentration of 100 $\mu\text{g}/\text{ml}$ prior to suspending cells and injecting into the molds. After removing gels from the molds, a 5-mm biopsy punch was used to core out samples that were 2 mm in height. All cell constructs were placed in 12-well transwell and cultured with culture media for 28 days, with the media changed every 2 days.

3.2.2 Cell Viability

After 28 days of culture, the media was aspirated and constructs were removed from the transwells and cut in half using a sterilized scalpel. One half was frozen down at -20°C and saved for biochemistry (Section 3.2.3) and the other half was immediately placed in Labtek chambered cover glass slides (Fisher Scientific). The sample was then submersed in a LIVE/DEAD staining solution (2 mM ethidium homodimer-1 and 4 mM calcein AM in 1X PBS; Molecular Probes; Eugene, OR) for 30 minutes at 23°C. All

samples were rinsed with 1X PBS before imaging (n=4). Live cells were identified by green fluorescence and dead cells by red fluorescence.

Laser scanning confocal microscopy (Plan-Neofluar 10X objective, confocal slice thickness = 20 μ m) was used to image porcine NP cells stained with LIVE/DEAD assay reagents. Three images were taken throughout the gel at different depths. These images were analyzed using Nikon image analysis software to count the number of live cells as a percentage of the total number of cells in the image. The percentages were averaged to obtain a single data point (n=4).

3.2.3 Biochemistry

After 28 days of culture, each construct half was weighed and lyophilized for 16 hours. Samples of PEGDA containing no cells were also lyophilized and served as negative controls. After lyophilization, the samples were cut into smaller pieces using a scalpel and then ground using a microtube pestle (USA Scientific; Ocala, FL). All samples and controls were digested in 300 μ g/mL of papain (Sigma) solution prepared in 1X PBS containing 5 mM EDTA (Mallinckrodt; Hazelwood, MO) and 5 mM cysteine-HCl anhydrous (Sigma). Samples were digested in 1.0 mL of papain solution for 16 hours at 65°C and then stored at -80°C until further use.

3.2.3.1 Dimethylmethyle Blue (DMMB) Assay

Aliquots of papain-digested samples and controls were thawed and mixed on a vortex mixer before being analyzed for sulfated-glycosaminoglycan (sGAG) content via the DMMB assay. Samples and controls were incubated with the dye solution (pH = 3) in a 96-well assay plate. Absorbances were read at 540 nm on a Tecan plate reader (GENios, Phenix Research Systems; Candler, NC) and sGAG content was calculated from a standard curve prepared from commercial chondroitin-4-sulfate (Calbiochem; La Jolla, CA). The mean absorbance for each acellular counterpart was subtracted from the matching cellular counterpart for final determination of total sGAG content. The values for each sample were normalized by its respective wet weight.

3.2.3.2 Sircol Collagen Assay

All papain-digested samples were thawed and vortexed before being analyzed for collagen content using the Sircol Collagen Assay Kit (Biocolor; Northern Ireland, UK). All samples and controls were incubated with the Sircol Dye reagent for 30 minutes, where each sample was gently mixed every 5 minutes. Samples were then centrifuged at 10,000 g for 10 minutes to collect the collagen-bound dye and the supernatant was removed. The pellet was resuspended in the Alkali reagent provided in the kit, and samples were transferred to a 96-well assay plate. Absorbances were read at 540 nm on a Tecan plate reader (GENios, Phenix Research Systems) and total collagen

content was calculated from a standard curve prepared from assay kit provided soluble type I collagen. The mean absorbance for each acellular counterpart was subtracted from the matching cellular counterpart for final determination of total collagen content. The values for each sample were normalized by its respective wet weight.

3.2.4 Mechanical Testing

After 28 days of culture, all samples were removed from culture and rinsed with 1X PBS. On the day of testing, sample diameters of each construct were determined using high-resolution, digital photographs. Unconfined compression tests were performed on an AR-G2 rheometer and software (TA Instruments; New Castle, DE) in a parallel plate configuration (nonporous stainless steel platens, radius = 8 mm). All test samples were submerged in cell culture media in a temperature controlled bath at 37°C. All samples were subjected to three cycles of preconditioning. For each cycle, an initial force of 0.03 N was applied for 3 minutes. The reference thickness of each sample was recorded as the distance between the platens under a 0.02 N compressive tare load after preconditioning. Samples were compressed to a 5% compressive strain at a rate of 0.01 mm/s and then allowed to relax for 1 hour, which was enough time in preliminary studies to achieve complete relaxation. This was repeated in 5% increments until 20% strain was achieved, allowing for 60 minutes of relaxation after each incremental strain was applied. Load and displacement data were recorded every 5 seconds.

The last ten data points at the end of each relaxation period were averaged to obtain the stress value at equilibrium for each applied strain value. Stress values were plotted against strain for each amount of applied strain and a linear regression was performed to obtain the slope of the line, which is the equilibrium compressive modulus of each cell construct.

3.2.5 Histology

Immediately following mechanical testing, all samples were embedded in OCT medium and flash frozen in liquid nitrogen. A cryostat was used to obtain 10- μ m frozen sections. All sections were stored at -80°C until further use. Frozen sections were oven-dried at 60°C for 30 minutes before staining. Sections were then fixed in 10% neutral-buffered formalin (Azer Scientific; Morgantown, PA) for 10 minutes.

3.2.5.1 Safranin-O Staining

One section per construct was counterstained with Mayer hematoxylin (Sigma) for 15 minutes, rinsed in warm tap water for 15 minutes and distilled water for 30 seconds. Sections were then washed in 1% lithium carbonate solution (Mallinckrodt Chemicals; Phillipsburg, NJ) and stained with safranin-O solution (Sigma) for 60 seconds. Samples were rinsed with distilled water, and subsequently dehydrated with 190 proof ethanol (Koptec; King of Prussia, PA), 200 proof ethanol (Koptec) and xylene

substitute (Sigma). Sections were then mounted with Permount (Fisher Scientific) and visualized with light microscopy.

3.2.5.2 Collagen Immunohistochemistry

Two sections per construct were processed for immunohistochemical labeling of types I and II collagen using the HistoStain Plus Broad Spectrum staining kit (Invitrogen). To label type I collagen, samples were incubated in a peroxo-block solution for 45 minutes at room temperature, washed in 1X PBS and incubated with blocking serum for 30 minutes at 4°C (Reagent A in HistoStain kit). Primary antibody (C2456 monoclonal anti-collagen, type I; Sigma) was then added to the slides at a dilution of 1:300 in Reagent A for 120 minutes at 4°C. This antibody was produced against type I collagen from bovine skin, but is reactive with porcine tissue (Sigma). Following washing with PBS, sections were incubated with secondary antibody (Reagent B in HistoStain kit) at a dilution of 1:1 in Reagent A for 30 minutes at room temperature, washed with PBS, and incubated with enzyme conjugate (Reagent C in HistoStain kit) for 30 minutes at room temperature, washed again with PBS, and incubated with substrate-chromagen mixture (Reagent D in HistoStain kit), which results in a deep red color, for 10 minutes at room temperature. Sections were washed in distilled water, and counterstained with Mayer's Hematoxylin to visualize individual cells and mounted in GVA mounting medium (Sigma).

Sections stained for type II collagen followed the same protocol with an additional digestion step. Following peroxo-blocking, sections were digested with pepsin (Digest-All 3; Invitrogen) for 20 minutes at 37°C. This enzyme will help expose the type II collagen epitope recognized by the II-II6B3 primary antibody (diluted 1:300; Developmental Studies Hybridoma Bank, Iowa City, IA). Negative controls of acellular PEGDA gels were processed for type I and II collagen in parallel with the omission of the primary antibodies.

3.2.8 Statistical Analysis

Data are presented as the mean \pm SEM ($n = 4$). A one-way ANOVA was used to determine the effect of cell viability, ECM production (normalized type I and II collagen and sGAG content), and equilibrium compressive modulus. Pairwise comparisons were made using a Student t-test and significance was set at $p < 0.05$. Statistical analyses were performed using JMP software (SAS Institute; Cary, NC).

3.3 Results

All agarose cell-constructs were unable to maintain their structural integrity after 28 days of culture and were unable to be processed for analysis. All results presented were obtained from PEGDA gels with and without 100 $\mu\text{g/mL}$ of LM-111.

3.2.1 Cell Viability

Cell constructs containing entrapped LM-111 exhibited higher levels of cell survival and viability over 28 days of culture in PEGDA gels (Figure 8). The percentage of live cells in the absence of LM-111 was 12.1%, and with LM-111 was 31.4% (Figure 9).

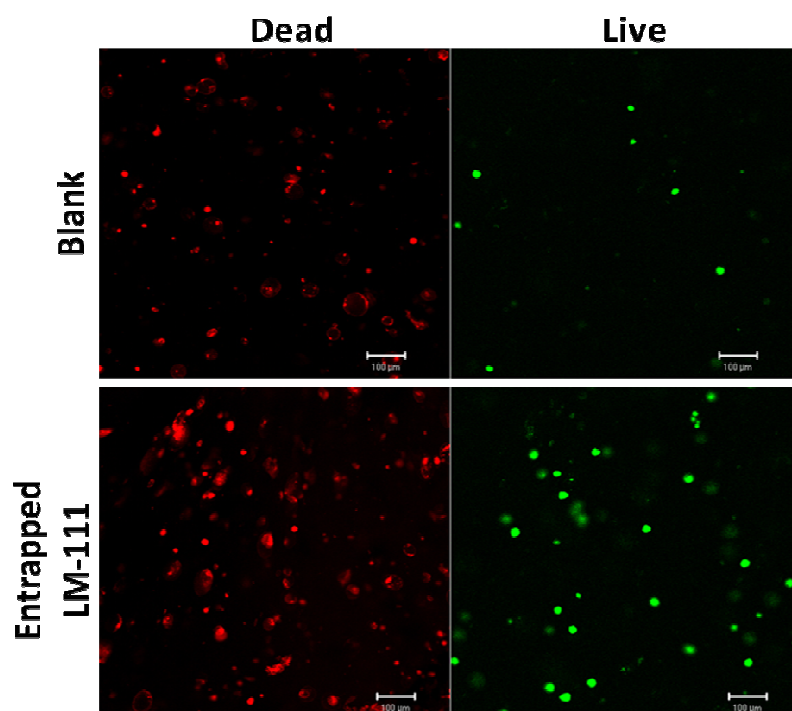


Figure 8: Live/Dead images of NP cells cultured in PEGDA gels with (bottom row) or without LM-111 (top row).

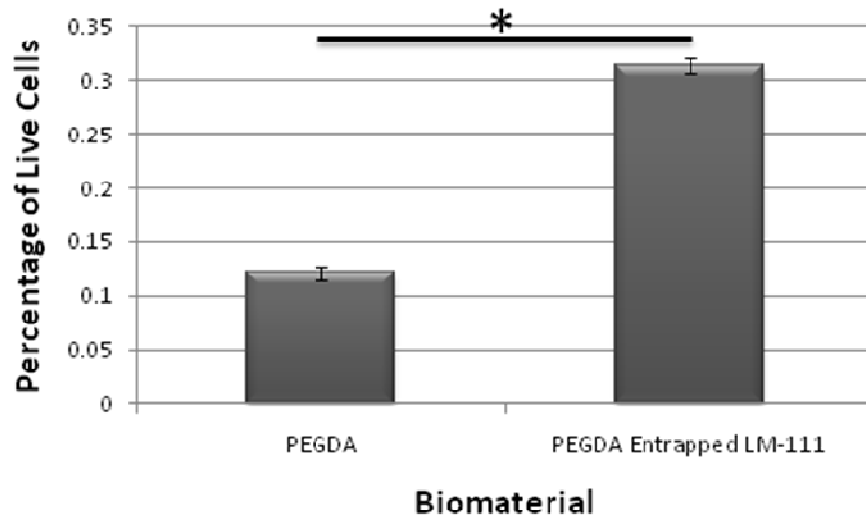


Figure 9: Percentage of live NP cells cultured in PEGDA gels with or without 100 µg/ml of LM-111. Data (mean ± SEM) show results from 4 independent experiments. * $p = 0.0025$.

3.3.2 Extracellular Matrix (ECM) Production

Histological staining revealed a higher amount type I collagen in comparison to type II collagen for PEGDA and PEGDA with LM-111 cultures. In contrast, porcine NP tissue s stained intensely for type II collagen, but not for type I collagen (Figure 10). Acellular negative controls were transparent with no evidence of cellular infiltration or matrix accumulation (not shown). A quantitative analysis from Sircol Collagen Assay results revealed no significant differences in levels of collagen production between culture conditions ($p = 0.2218$; Figure 13). Although the Sircol Assay does not differentiate amongst the different collagen types, histological images reveal that the type I collagen is the major collagen component in the ECM of cell-constructs.

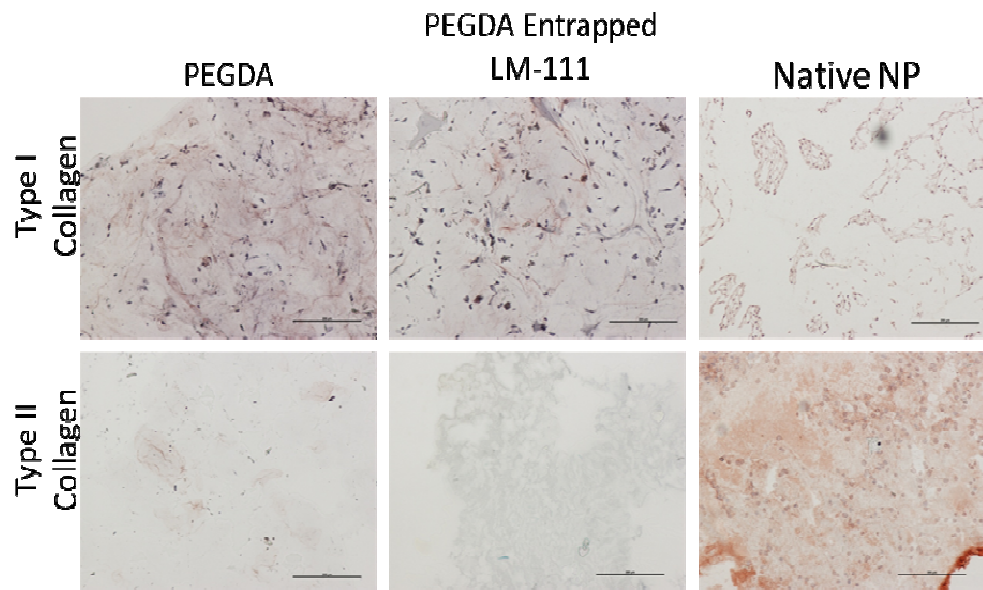


Figure 10: Representative histological images of PEGDA tissue construct with and without LM-111 and native NP tissue stained with type I and II collagen. Scale bars = 200 μ m.

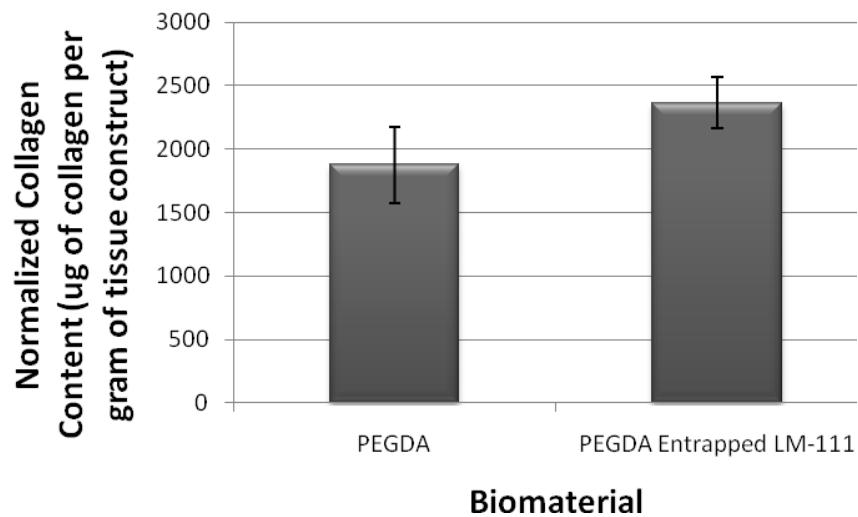


Figure 11: Collagen content levels normalized to total wet weight of tissue construct. Data shown (mean \pm SEM) are results from 4 independent experiments.

Safranin-O images revealed high intensity staining for both the PEGDA material (Figure 12, B) and the ECM of the native NP tissue (Figure 12, C). These results indicate that safranin-O binds intensely to sGAG content as well as the PEGDA itself. Histological images of PEGDA and PEGDA with LM-111 sections stained intensely with safranin-O (Figure 12, C and D), but sGAG content cannot be determined from histology alone. A quantitative analysis from DMMB assay demonstrated very low amounts of sGAG content in cell-constructs (Figure 13), which suggests that the majority of the staining seen in safranin-O images is due to the PEGDA. Furthermore, DMMB results revealed no significant differences between total sGAG content in PEGDA and PEGDA with LM-111 gels ($p = 0.5237$; Figure 13).

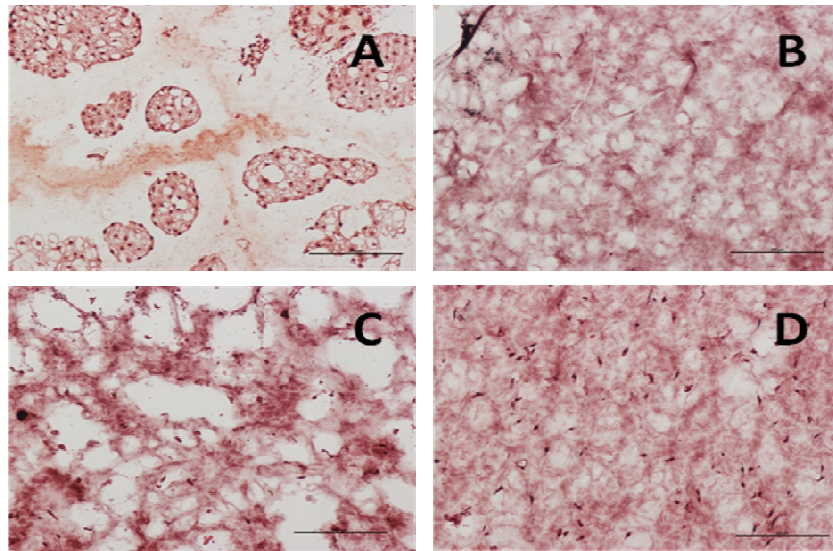


Figure 12: Representative safranin-O images of A) native NP tissue, B) acellular PEGDA, C) NP cells cultured in PEGDA gels for 28 days, D) NP cells cultured in PEGDA with 100 µg/ml of LM-111 for 28 days. Scale bars are 200 µm.

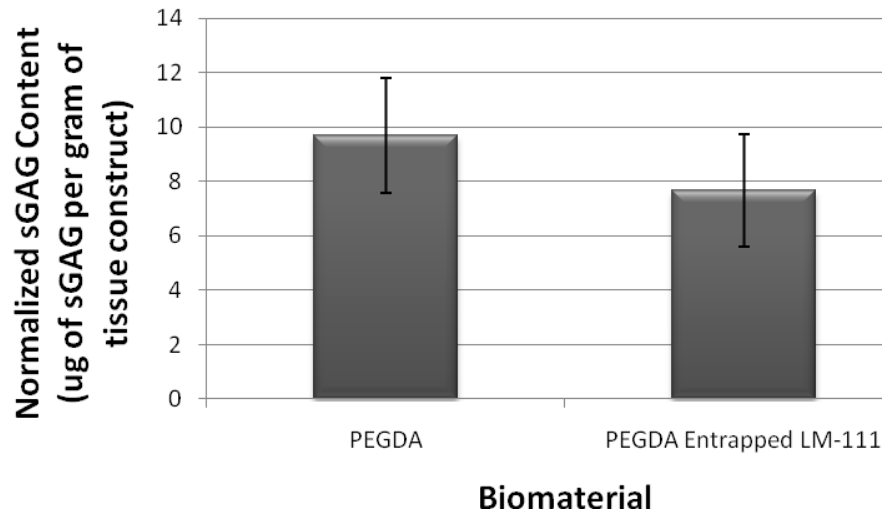


Figure 13: sGAG content levels normalized to total wet weight of tissue construct. Data shown (mean \pm SEM) are results from 4 independent experiments.

3.3.3 Mechanical Properties

The equilibrium compressive modulus of each PEGDA cell construct was measured after 28 days of culture. The compressive modulus was found to be 9.08 ± 1.96 kPa (mean \pm SEM) for cell constructs in blank PEGDA gels and 6.68 ± 2.95 kPa for cell constructs in PEGDA gels entrapped with LM-111 (Figure 14). Reported literature values for healthy human NP tissue under unconfined compression is 5.39 ± 2.56 kPa [54]. Results show no significant difference between PEGDA cell constructs with and without LM-111 ($p = 0.3069$).

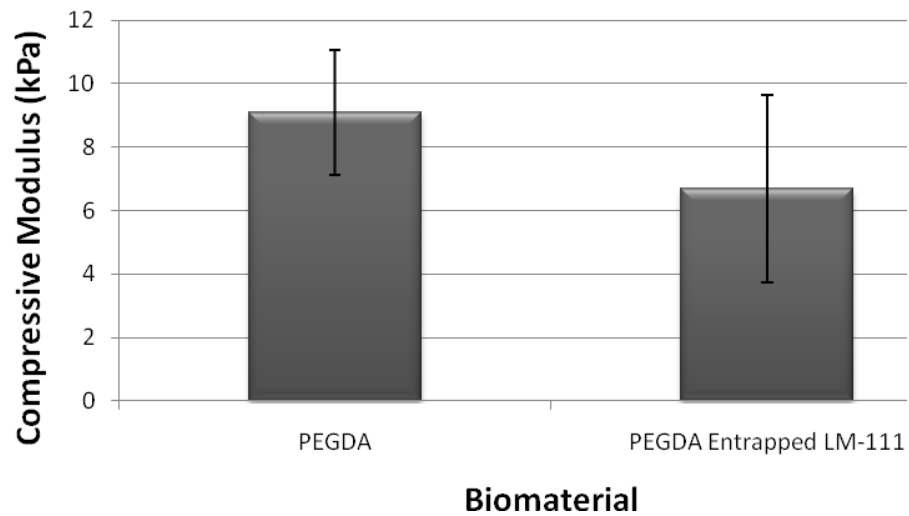


Figure 14: Compressive modulus of PEGDA cell-constructs with and without LM-111. Data shown (mean \pm SEM) are results from 3 independent experiments

3.4 Discussion

3.4.1 Long-Term Culture in Agarose Gels

Agarose has been used in many tissue engineering applications as a three-dimensional scaffold. It has been shown to support neurite extension *in vitro* [55, 62] and promote IVD disc cell survival [25-27]. In this current study, 2% agarose and 5% PEGDA were used to encapsulate porcine NP cells. After 28 days of culture, all agarose samples underwent complete dissolution, which prevented further assessment of these samples. All PEGDA samples maintained their structural integrity after 28 days of culture. Many previous investigations using agarose used relatively lower cell densities (1×10^6

cells/mL) than that used in this present study (10×10^6 cells/mL). The higher cell-seeding density was hypothesized to facilitate in the formation of cell clusters in a 3D culture, which have been shown to be crucial for normal NP cell function [68]. However, it is possible that the high density of cells interfered with the formation of crosslinks between agarose monomers, thus accelerating the rate of dissolution during culture.

The ability of agarose to maintain its structural integrity over longer term culture has not been well-characterized. Many of the studies reported in the literature that used agarose to entrap and culture cells were only carried out for 2 weeks. Chou *et al.* evaluated the capability of both ionically crosslinked and photocrosslinked alginate, a polysaccharide material that is similar to agarose, to support bovine NP cell culture for 28 days [24]. They showed that all of ionically crosslinked alginate severely dissociated after 28 days of culture *in vivo*, and were unable to be processed for biochemical analysis. Furthermore, NP cells demonstrated higher levels of cell viability and type II collagen production culture *in vitro* in photocrosslinked hydrogels than in ionically crosslinked hydrogels [24]. The findings from the literature and the results from this present study suggest that the method of crosslinking plays an important role in maintaining the structural integrity of the biomaterial for long-term culture *in vitro* or *in vivo* implantation.

Although all agarose samples severely dissolved after 28 days of culture, it is still of great interest to pursue the use of naturally-derived polymers because they mimic the negatively charged polysaccharides in cartilaginous tissues. Some research groups have modified various polysaccharides, including alginate [24, 50], hyaluronan acid [70] and carboxymethylcellulose [51] by incorporating a methacrylate or diacrylate group that can undergo radical polymerization upon exposure to ultraviolet radiation. These materials may offer greater advantages for NP tissue engineering applications than a biologically inert material such as PEG. Future directions involving photocrosslinkable polysaccharides will allow us to assess the intrinsic properties of the polymer itself, rather than the crosslinking method, to support NP cell survival and function.

3.4.2 Effect of Laminin-111 on NP Cell Behavior

The cell viability of NP cells was assessed in PEGDA cell constructs with and without LM-111 after 28 days of culture. Results from LIVE/DEAD assay revealed that the majority of cells were found to be dead even in the presence of LM-111. These results are consistent with the findings of other groups that have reported decreasing cell viability over 14 days for bovine NP cells encapsulated in photocrosslinked alginate [50] and for articular chondrocytes in photocrosslinked PEGDA [71]. However, LM-111 significantly increased cell viability when physically entrapped in PEGDA at a concentration of 100 $\mu\text{g/ml}$. This finding suggests the importance of incorporating

biological cues in an inert hydrogel environment to improve cell function. Therefore, cell viability may be further enhanced at higher concentrations of physically entrapped LM-111, or in combination with other laminin isoforms previously identified to influence NP cell function, such as LM-511 [15, 16]. Future work will focus on long-term maintenance of cell viability with the incorporation of degradation sites in the biomaterial, increased concentrations of ECM molecules, addition of growth factors to optimize culture medium and/or mechanical stimulation.

Due to the severe compromise in cell viability after 28 days of culture, no information could be obtained regarding the cell morphology and protein expression of NP cells cultured in PEGDA gels. However, there exists strong evidence in the literature that NP cell behavior is influenced by specific laminin ligands when cultured on a 2D substrate [15, 16]. Furthermore, this study demonstrated that LM-111 can promote greater cell viability of porcine NP cells than in a 3D PEGDA environment. However, it remains unclear whether LM-111 can promote NP cells to remain in the notochordal-like cell phenotype that is characteristic of the cell population in immature NP tissues. Future work will include visualizing the actin cytoskeleton to assess the morphology of NP cells cultured in hydrogels in response to LM-111 and LM-511, which is another laminin isoform that has been shown to be present in the immature NP. Several studies have identified protein markers, including CD44s, galectin 3, cytokeratin 8, and

vimentin, that are specifically expressed in the notochordal NP cells and not in the chondrocytic NP cells that are found in mature NP tissues [72]. Notochordal NP cells also express a much higher proteoglycan to collagen ratio than cartilage cells [73, 74]. The relationship between expression of these protein markers and their function in the NP is even less understood than the NP cell phenotype, but the identification of specific cell-matrix interactions between certain laminin isoforms and their receptors may provide important insight into the role of notochordal cells in the maintenance of a healthy NP tissue. Therefore, future work will include assessing the expression of LM-111 subchains and the receptors that specifically interact with those subunits, including $\alpha 3$, $\alpha 6$, and $\beta 1$ integrin subunits, CD239 and CD151 [15-17].

3.4.3 PEGDA-Laminin Cell Constructs for NP Tissue Replacement

One of the important factors in a tissue engineering NP construct is the production of proteoglycans, which is believed to significantly contribute to the mechanical properties of the IVD. Results show no significant difference in ECM production for NP cells encapsulated in blank PEGDA gels and PEGDA gels with 100 $\mu\text{g/ml}$ of entrapped LM-111. It is possible that LM-111 at the given concentration has no effect on ECM production over 28 days. Additionally, the presence of serum in the cell culture medium may be the dominant factor in driving long term effects such as matrix production and accumulation. Thus, any effect of the LM-111 is completely masked by

the serum in the medium. This result is supported by evidence of the higher accumulation of type I collagen than type II collagen or sGAG in the pericellular matrix, which suggests that the cells are losing their NP cell phenotype and becoming more chondrocyte-like in response to the serum. Culturing NP cells with higher concentrations of LM-111 or different laminin isoforms either in the biomaterial or in the medium may reverse the differentiation effects of the serum or allow the cells to produce a more NP-like matrix *in vitro*.

Several studies have demonstrated that the crosslinking density and rigidity of the hydrogel may prevent elaboration and remodeling of the ECM, which in turn may affect the cell viability and activity [75, 76]. While histological images and biochemistry revealed some ECM production and accumulation, the levels of the sGAG production in both PEGDA constructs are four orders of magnitude lower than reported sGAG levels in sheep NP tissue ($20.88 \pm 4.82 \mu\text{g}/\text{mg}$ of tissue) [77]. Additionally, results from the LM-111 entrapment study in Section 2.3 demonstrate low levels of entrapment in a 5% (w/v) PEGDA gel. Thus, it is highly likely that using a PEGDA with a molecular weight of 10 kDa is preventing NP cells from synthesizing an appropriate matrix that can support healthy cell function. Subsequent studies will involve characterizing the effect of PEGDA monomer molecular weight and weight percent of gels on NP cell function. Furthermore, the non-degradable nature of the PEGDA polymer may be hindering NP

cell function, suggesting that a tissue engineering construct would benefit from incorporating degradable units into the polymer backbone by allowing NP cells to remodel their ECM environment. These degradable units may be another polymeric monomer [78], an enzymatically cleavable peptide sequences or even a full-length protein [21, 64].

The incorporation of degradable units may also improve the mechanical properties of the PEGDA constructs. Results demonstrated LM-111 had no significant affect on ECM accumulation and the equilibrium compressive modulus of cell constructs. However, both construct conditions were much stiffer than both native human NP tissue [54] and other studies that implanted encapsulated bovine NP cells in alginate for 8 weeks [24]. Preliminary studies of 2 week cultures of porcine NP cells in PEGDA gels revealed the compressive modulus to be approximately 4 kPa (data not shown), which is much closer to the value of the native NP tissue. This finding suggests that the cell constructs are increasing in stiffness over time due to increased ECM accumulation. However, the NP cell phenotype may be lost due to the extended culture time in serum-containing medium, leading to a higher production and accumulation of type I collagen. This will result in a construct that is stiffer than the NP tissue. Additionally, the shift from a population of highly-vacuolated cells to smaller chondrocytic cells may account for the increase in compressive modulus. To understand

the contribution of the hydrogel network alone to the mechanical properties of the cell construct, a separate study must investigate the compressive modulus of acellular PEGDA gels at various monomer concentrations and molecular weights. In addition, characterizing the shear modulus and Poisson's ratio will provide more extensive assessing the mechanical properties of the PEGDA cell constructs to serve as a viable NP replacement.

3.5 Conclusions

The results from this chapter provided a better understanding of porcine NP cell behavior and function in three-dimensional hydrogels for long-term cultures *in vitro*. Furthermore, the incorporation of ECM molecules, such as LM-111, may be beneficial for promoting cell viability. Major conclusions from these studies include:

1. **Unmodified agarose is not suitable material for long term culture.** Due to severe dissolution of all agarose cell constructs throughout culture, Hypothesis 3.A could not be evaluated. A more stable system involving photocrosslinkable polysaccharide material, such as hyaluronan modified with diacrylate groups, will be necessary to assess the effect of scaffolding biomaterial on NP cell function.
2. **LM-111 did not promote the synthesis of an NP-like matrix in a PEGDA hydrogel environment, which rejects Hypothesis 3.B.** Results revealed an

increase in type I collagen in the ECM and higher values of compressive modulus than native human NP tissue. The rigidity and non-degradable nature of PEGDA may inhibit normal ECM remodeling.

3. **LM-111 promoted higher levels of cell viability over 28 days of culture, which supports Hypothesis 3.C.** However, the majority of cells were nonviable, even with LM-111, which suggests that incorporation of a different laminin isoform, such as LM-511, or degradable sites in the biomaterial may be necessary to maintain proper NP cell function.

4. Conclusions and Future Directions

The nucleus pulposus (NP) is a soft, hydrated tissue in the intervertebral disc (IVD) that swells in response to mechanical loads applied to the spine. It undergoes dramatic biochemical and mechanical changes with age and degeneration. The most notable changes include decreased synthesis of proteoglycans, which subsequently leads to loss of water content, decreased disc height, and loss of functionality due to its inability to maintain a high swelling pressure. This loss of proteoglycan content has been found to coincide with the disappearance of the large, highly-vacuolated cells that have been identified in the NP and are believed to have originated from the notochord region. It is believed that the notochordal-like cells are responsible for synthesizing the proteoglycan-rich matrix that is responsible for the fluidity of the NP. Previous work in our lab has identified specific ECM molecules that may be important for the maintenance of this immature cell type in the NP. These molecules include specific laminin isoforms, LM-111 and LM-511, and their associated receptors that are uniquely expressed in the immature NP. The objective of this project was to present one of the key ECM molecules, LM-111, in a 3D hydrogel biomaterial and assess the ability of those conditions to provide a viable 3D platform for engineering an NP tissue replacement.

The studies from Chapter 2 demonstrate that full-length LM-111 protein can be physically entrapped in the hydrogel networks of agarose, alginate and polyethylene

glycol diacrylate (PEGDA). Results indicate that agarose may be the most suitable for entrapping large ECM molecules such as LM-111 as immunostaining images revealed the highest intensity for staining of LM-111 in frozen agarose sections. However, future studies will investigate the bioactivity of LM-111 when entrapped in the 3D hydrogel environment.

Increase cell survival of NP cells after 28 days of culture, presented in Chapter 3, suggest that LM-111 retained at least some of its biological activity when entrapped in PEGDA gels. Agarose-cell constructs were not able to maintain its structural integrity during long-term culture of NP cells, and could not be assessed for biological activity. Nonetheless, this finding allows us to understand the importance of crosslinking method when designing a 3D tissue culture platform. Photocrosslinked hydrogels may be more beneficial for long-term cultures or *in vivo* cultures because it forms crosslinks that can remain stable throughout culture.

Assessment of ECM production and mechanical properties of NP cells cultured in PEGDA gels for 28 days revealed no effect of LM-111 in promoting the synthesis of a functional NP-like matrix. It is possible that the concentration of LM-111 used in this study was insufficient to elicit any significant changes in NP cell behavior, especially when cultured in serum-containing culture medium. Additionally, future studies will incorporate degradable units into the hydrogel polymer backbone to allow NP cells to

remodel their surrounding matrix. The inability of NP cells to deposit a functional matrix may explain the increase equilibrium compressive modulus of the PEGDA-cell constructs compared to native human NP tissue. The inclusion of degradable units may improve the matrix synthesis of NP cells and provide a more functional tissue for NP replacement. Furthermore, the synthesis of a more NP-like matrix may promote greater cell survival and proliferation.

In summary, the major findings in this work suggest that NP cells do respond to LM-111 in a 3D environment. Previous work with NP cells in 2D has suggested a more important role of LM-111 to maintain notochordal-like phenotype in addition to promoting cell survival. Thus, future work will focus on improving culture conditions and the properties of the hydrogel to further enhance cell survival during long-term culture. Providing a platform that can be degraded and remodeled by NP cells will be crucial to improve NP cell behavior in response to LM-111. Additionally, future studies should include other important laminin isoforms such as LM-511 into the hydrogel environment or growth factors such as TGF- β , which has been shown to promote matrix production in disc cells [25], into the cell culture medium. Overall, the results from this project suggest potential for the use of hydrogel biomaterials that can present important biological cues, such as ECM molecules, to regenerate a viable, NP tissue replacement.

References

1. Humzah, M. and R. Soames, *Human intervertebral disc: structure and function*. The Anatomical Record, 1988. **220**(4): p. 337-356.
2. O'Halloran, D. and A. Pandit, *Tissue-engineering approach to regenerating the intervertebral disc*. Tissue engineering, 2007. **13**(8): p. 1927-1954.
3. Zhao, C., et al., *The cell biology of intervertebral disc aging and degeneration*. Ageing research reviews, 2007. **6**(3): p. 247-261.
4. Erwin, W.M., *The enigma that is the nucleus pulposus cell: the search goes on*. Arthritis Res Ther, 2010. **12**(3): p. 118.
5. Erwin, W.M. and R.D. Inman, *Notochord cells regulate intervertebral disc chondrocyte proteoglycan production and cell proliferation*. Spine (Phila Pa 1976), 2006. **31**(10): p. 1094-9.
6. Gilson, A., M. Dreger, and J.P. Urban, *Differential expression level of cytokeratin 8 in cells of the bovine nucleus pulposus complicates the search for specific intervertebral disc cell markers*. Arthritis Res Ther, 2010. **12**(1): p. R24.
7. Risbud, M.V., T.P. Schaer, and I.M. Shapiro, *Toward an understanding of the role of notochordal cells in the adult intervertebral disc: from discord to accord*. Dev Dyn, 2010. **239**(8): p. 2141-8.
8. Kim, K., et al., *The origin of chondrocytes in the nucleus pulposus and histologic findings associated with the transition of a notochordal nucleus pulposus to a fibrocartilaginous nucleus pulposus in intact rabbit intervertebral discs*. Spine, 2003. **28**(10): p. 982.
9. Weber, L.M., K.N. Hayda, and K.S. Anseth, *Cell-matrix interactions improve beta-cell survival and insulin secretion in three-dimensional culture*. Tissue Eng Part A, 2008. **14**(12): p. 1959-68.
10. Hynes, R.O., *Integrins: bidirectional, allosteric signaling machines*. Cell, 2002. **110**(6): p. 673-87.
11. Knudson, W. and R. Loeser, *CD44 and integrin matrix receptors participate in cartilage homeostasis*. Cellular and Molecular Life Sciences, 2002. **59**(1): p. 36-44.

12. Ostergaard, K., et al., *Expression of and subunits of the integrin superfamily in articular cartilage from macroscopically normal and osteoarthritic human femoral heads*. *Annals of the rheumatic diseases*, 1998. **57**(5): p. 303.
13. Salter, D., et al., *Integrin expression by human articular chondrocytes*. *Rheumatology*, 1992. **31**(4): p. 231.
14. Xia, M. and Y. Zhu, *Expression of integrin subunits in the herniated intervertebral disc*. *Connect Tissue Res*, 2008. **49**(6): p. 464-9.
15. Chen, J., et al., *Expression of laminin isoforms, receptors, and binding proteins unique to nucleus pulposus cells of immature intervertebral disc*. *Connect Tissue Res*, 2009. **50**(5): p. 294-306.
16. Gilchrist, C.L., et al., *Functional integrin subunits regulating cell-matrix interactions in the intervertebral disc*. *J Orthop Res*, 2007. **25**(6): p. 829-40.
17. Nettles, D.L., W.J. Richardson, and L.A. Setton, *Integrin expression in cells of the intervertebral disc*. *J Anat*, 2004. **204**(6): p. 515-20.
18. Cruise, G., D. Scharp, and J. Hubbell, *Characterization of permeability and network structure of interfacially photopolymerized poly (ethylene glycol) diacrylate hydrogels*. *Biomaterials*, 1998. **19**(14): p. 1287-1294.
19. Bryant, S., C. Nuttelman, and K. Anseth, *Cytocompatibility of UV and visible light photoinitiating systems on cultured NIH/3T3 fibroblasts in vitro*. *Journal of Biomaterials Science, Polymer Edition*, 2000. **11**(5): p. 439-457.
20. Hwang, N., S. Varghese, and J. Elisseeff, *Cartilage tissue engineering: Directed differentiation of embryonic stem cells in three-dimensional hydrogel culture*. *Methods in molecular biology (Clifton, NJ)*, 2007. **407**: p. 351.
21. Peled, E., et al., *A novel poly (ethylene glycol)–fibrinogen hydrogel for tibial segmental defect repair in a rat model*. *Journal of Biomedical Materials Research Part A*, 2007. **80**(4): p. 874-884.
22. Weber, L., C. Lopez, and K. Anseth, *Effects of PEG hydrogel crosslinking density on protein diffusion and encapsulated islet survival and function*. *Journal of Biomedical Materials Research Part A*, 2009. **90**(3): p. 720-729.

23. Baer, A.E., et al., *Collagen gene expression and mechanical properties of intervertebral disc cell-alginate cultures*. J Orthop Res, 2001. **19**(1): p. 2-10.
24. Chou, A.I., S.O. Akintoye, and S.B. Nicoll, *Photo-crosslinked alginate hydrogels support enhanced matrix accumulation by nucleus pulposus cells in vivo*. Osteoarthritis Cartilage, 2009. **17**(10): p. 1377-84.
25. Gruber, H.E., et al., *Human intervertebral disc cells from the annulus: three-dimensional culture in agarose or alginate and responsiveness to TGF-beta1*. Exp Cell Res, 1997. **235**(1): p. 13-21.
26. Gruber, H.E., et al., *Three-dimensional culture of human disc cells within agarose or a collagen sponge: assessment of proteoglycan production*. Biomaterials, 2006. **27**(3): p. 371-6.
27. Gruber, H.E., et al., *Cell-based tissue engineering for the intervertebral disc: in vitro studies of human disc cell gene expression and matrix production within selected cell carriers*. Spine J, 2004. **4**(1): p. 44-55.
28. Sebastine, I.M. and D.J. Williams, *Current developments in tissue engineering of nucleus pulposus for the treatment of intervertebral disc degeneration*. Conf Proc IEEE Eng Med Biol Soc, 2007. **2007**: p. 6401-6.
29. Wang, J.Y., et al., *Intervertebral disc cells exhibit differences in gene expression in alginate and monolayer culture*. Spine (Phila Pa 1976), 2001. **26**(16): p. 1747-51; discussion 1752.
30. Bogduk, N., *Clinical anatomy of the lumbar spine and sacrum*. 2005: Churchill Livingstone.
31. Elliott, D. and L. Setton, *A linear material model for fiber-induced anisotropy of the annulus fibrosus*. Journal of biomechanical engineering, 2000. **122**: p. 173.
32. Cappello, R., et al., *Notochordal cell produce and assemble extracellular matrix in a distinct manner, which may be responsible for the maintenance of healthy nucleus pulposus*. Spine, 2006. **31**(8): p. 873.
33. Nomura, T., et al., *Nucleus pulposus allograft retards intervertebral disc degeneration*. Clinical orthopaedics and related research, 2001. **389**: p. 94.

34. Aguiar, D., S. Johnson, and T. Oegema, *Notochordal Cells Interact with Nucleus Pulposus Cells: Regulation of Proteoglycan Synthesis** 1. *Experimental cell research*, 1999. **246**(1): p. 129-137.
35. Errington, R.J., et al., *Characterisation of cytoplasm-filled processes in cells of the intervertebral disc*. *J Anat*, 1998. **192 (Pt 3)**: p. 369-78.
36. Guilak, F., et al., *Viscoelastic properties of intervertebral disc cells. Identification of two biomechanically distinct cell populations*. *Spine (Phila Pa 1976)*, 1999. **24**(23): p. 2475-83.
37. Johnson, W.E. and S. Roberts, *Human intervertebral disc cell morphology and cytoskeletal composition: a preliminary study of regional variations in health and disease*. *J Anat*, 2003. **203**(6): p. 605-12.
38. Li, S., V.C. Duance, and E.J. Blain, *Zonal variations in cytoskeletal element organization, mRNA and protein expression in the intervertebral disc*. *J Anat*, 2008. **213**(6): p. 725-32.
39. Kikkawa, Y., et al., *Integrin binding specificity of laminin-10/11: laminin-10/11 are recognized by alpha 3 beta 1, alpha 6 beta 1 and alpha 6 beta 4 integrins*. *J Cell Sci*, 2000. **113 (Pt 5)**: p. 869-76.
40. Miner, J.H. and P.D. Yurchenco, *Laminin functions in tissue morphogenesis*. *Annu Rev Cell Dev Biol*, 2004. **20**: p. 255-84.
41. Nishiuchi, R., et al., *Ligand-binding specificities of laminin-binding integrins: a comprehensive survey of laminin-integrin interactions using recombinant alpha3beta1, alpha6beta1, alpha7beta1 and alpha6beta4 integrins*. *Matrix Biol*, 2006. **25**(3): p. 189-97.
42. Chen, J., W. Yan, and L.A. Setton, *Molecular phenotypes of notochordal cells purified from immature nucleus pulposus*. *Eur Spine J*, 2006. **15 Suppl 3**: p. S303-11.
43. Hohaüs, C., et al., *Cell transplantation in lumbar spine disc degeneration disease*. *European spine journal*, 2008. **17**: p. 492-503.
44. Le Visage, C., et al., *Interaction of human mesenchymal stem cells with disc cells: changes in extracellular matrix biosynthesis*. *Spine*, 2006. **31**(18): p. 2036.

45. Okuma, M., et al., *Reinsertion of stimulated nucleus pulposus cells retards intervertebral disc degeneration: an in vitro and in vivo experimental study*. Journal of Orthopaedic Research, 2000. **18**(6): p. 988-997.
46. Sakai, D., *Future perspectives of cell-based therapy for intervertebral disc disease*. European spine journal, 2008. **17**: p. 452-458.
47. Yamamoto, Y., et al., *Upregulation of the viability of nucleus pulposus cells by bone marrow-derived stromal cells: significance of direct cell-to-cell contact in coculture system*. Spine, 2004. **29**(14): p. 1508.
48. Bader, R. and W. Rochefort, *Rheological characterization of photopolymerized poly (vinyl alcohol) hydrogels for potential use in nucleus pulposus replacement*. Journal of Biomedical Materials Research Part A, 2008. **86**(2): p. 494-501.
49. Nguyen, K. and J. West, *Photopolymerizable hydrogels for tissue engineering applications*. Biomaterials, 2002. **23**(22): p. 4307-4314.
50. Chou, A. and S. Nicoll, *Characterization of photocrosslinked alginate hydrogels for nucleus pulposus cell encapsulation*. Journal of Biomedical Materials Research Part A, 2009. **91**(1): p. 187-194.
51. Reza, A. and S. Nicoll, *Characterization of novel photocrosslinked carboxymethylcellulose hydrogels for encapsulation of nucleus pulposus cells*. Acta Biomaterialia, 2010. **6**(1): p. 179-186.
52. Roughley, P., et al., *The potential of chitosan-based gels containing intervertebral disc cells for nucleus pulposus supplementation*. Biomaterials, 2006. **27**(3): p. 388-396.
53. Sakai, D., et al., *Atelocollagen for culture of human nucleus pulposus cells forming nucleus pulposus-like tissue in vitro: influence on the proliferation and proteoglycan production of HNPSV-1 cells*. Biomaterials, 2006. **27**(3): p. 346-353.
54. Cloyd, J., et al., *Material properties in unconfined compression of human nucleus pulposus, injectable hyaluronic acid-based hydrogels and tissue engineering scaffolds*. European spine journal, 2007. **16**(11): p. 1892-1898.
55. Bellamkonda, R., J. Ranieri, and P. Aebischer, *Laminin oligopeptide derivatized agarose gels allow three dimensional neurite extension in vitro*. Journal of neuroscience research, 1995. **41**(4): p. 501-509.

56. Weber, L., et al., *The effects of cell-matrix interactions on encapsulated [beta]-cell function within hydrogels functionalized with matrix-derived adhesive peptides*. Biomaterials, 2007. **28**(19): p. 3004-3011.
57. Graf, J., et al., *Identification of an amino acid sequence in laminin mediating cell attachment, chemotaxis, and receptor binding*. Cell, 1987. **48**(6): p. 989-996.
58. Jucker, M., H. Kleinman, and D. Ingram, *Fetal rat septal cells adhere to and extend processes on basement membrane, laminin, and a synthetic peptide from the laminin A chain sequence*. Journal of neuroscience research, 1991. **28**(4): p. 507-517.
59. Sephel, G., et al., *Laminin A chain synthetic peptide which supports neurite outgrowth*. Biochemical and biophysical research communications, 1989. **162**(2): p. 821-829.
60. Pinkse, G., et al., *Integrin signaling via RGD peptides and anti- 1 antibodies confers resistance to apoptosis in islets of Langerhans*. Diabetes, 2006. **55**(2): p. 312.
61. Wang, R. and L. Rosenberg, *Maintenance of beta-cell function and survival following islet isolation requires re-establishment of the islet-matrix relationship*. Journal of Endocrinology, 1999. **163**(2): p. 181.
62. Yu, X., G. Dillon, and R. Bellamkonda, *A laminin and nerve growth factor-laden three-dimensional scaffold for enhanced neurite extension*. Tissue engineering, 1999. **5**(4): p. 291-304.
63. Weber, L. and K. Anseth, *Hydrogel encapsulation environments functionalized with extracellular matrix interactions increase islet insulin secretion*. Matrix Biology, 2008. **27**(8): p. 667-673.
64. Schmidt, O., et al., *Immobilized fibrinogen in PEG hydrogels does not improve chondrocyte mediated matrix deposition in response to mechanical stimulation*. Biotechnology and bioengineering, 2006. **95**(6): p. 1061-1069.
65. Damodaran, G., et al., *Tethering a laminin peptide to a crosslinked collagen scaffold for biofunctionality*. J Biomed Mater Res A, 2009. **89**(4): p. 1001-10.
66. Iskakov, R., A. Kikuchi, and T. Okano, *Time-programmed pulsatile release of dextran from calcium-alginate gel beads coated with carboxy-n-propylacrylamide copolymers*. Journal of Controlled Release, 2002. **80**(1-3): p. 57-68.

67. Murray, M.M., et al., *The effect of thrombin on ACL fibroblast interactions with collagen hydrogels*. J Orthop Res, 2006. **24**(3): p. 508-15.
68. Hunter, C., J. Matyas, and N. Duncan, *The three dimensional architecture of the notochordal nucleus pulposus: novel observations on cell structures in the canine intervertebral disc*. Journal of anatomy, 2003. **202**(3): p. 279-291.
69. Trout, J., J. Buckwalter, and K. Moore, *Ultrastructure of the human intervertebral disc: II. Cells of the nucleus pulposus*. The Anatomical Record, 1982. **204**(4): p. 307-314.
70. Baier Leach, J., et al., *Photocrosslinked hyaluronic acid hydrogels: natural, biodegradable tissue engineering scaffolds*. Biotechnology and bioengineering, 2003. **82**(5): p. 578-589.
71. Elisseeff, J., et al., *Photoencapsulation of chondrocytes in poly (ethylene oxide)-based semi-interpenetrating networks*. Journal of Biomedical Materials Research Part A, 2000. **51**(2): p. 164-171.
72. Hunter, C., J. Matyas, and N. Duncan, *The notochordal cell in the nucleus pulposus: a review in the context of tissue engineering*. Tissue engineering, 2003. **9**(4): p. 667-677.
73. Mwale, F., P. Roughley, and J. Antoniou, *Distinction between the extracellular matrix of the nucleus pulposus and hyaline cartilage: a requisite for tissue engineering of intervertebral disc*. Eur Cell Mater, 2004. **8**: p. 58-63.
74. Yang, X. and X. Li, *Nucleus pulposus tissue engineering: a brief review*. European spine journal, 2009. **18**(11): p. 1564-1572.
75. Burdick, J., et al., *Controlled degradation and mechanical behavior of photopolymerized hyaluronic acid networks*. Biomacromolecules, 2005. **6**(1): p. 386-391.
76. Chung, C., et al., *Influence of gel properties on neocartilage formation by auricular chondrocytes photoencapsulated in hyaluronic acid networks*. Journal of Biomedical Materials Research Part A, 2006. **77**(3): p. 518-525.
77. Mizuno, H., et al., *Biomechanical and biochemical characterization of composite tissue-engineered intervertebral discs*. Biomaterials, 2006. **27**(3): p. 362-370.

78. Bryant, S. and K. Anseth, *Controlling the spatial distribution of ECM components in degradable PEG hydrogels for tissue engineering cartilage*. Journal of Biomedical Materials Research Part A, 2003. **64**(1): p. 70-79.